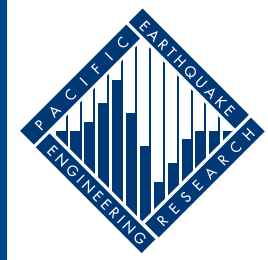

PACIFIC EARTHQUAKE ENGINEERING
RESEARCH CENTER

Statistics of SDF-System Estimate of Roof Displacement for Pushover Analysis of Buildings

Anil K. Chopra
Department of Civil and Environmental Engineering
University of California, Berkeley

Rakesh K. Goel
Department of Civil and Environmental Engineering
California Polytechnic State University, San Luis Obispo

Chatpan Chintanapakdee
Department of Civil and Environmental Engineering
University of California, Berkeley

A report on research conducted under Grant No. CMS-9812531 from the National Science Foundation: U.S.-Japan Cooperative Research in Urban Earthquake Disaster Mitigation

PEER 2001/16
DECEMBER 2001

Statistics of SDF-System Estimate of Roof Displacement for Pushover Analysis of Buildings

Anil K. Chopra
Professor
Department of Civil and Environmental Engineering
University of California, Berkeley

Rakesh K. Goel
Associate Professor
Department of Civil and Environmental Engineering
California Polytechnic State University, San Luis Obispo

Chatpan Chintanapakdee
Graduate Student
Department of Civil and Environmental Engineering
University of California, Berkeley

A report on research conducted under Grant No. CMS-9812531 from the National Science Foundation: U.S.-Japan Cooperative Research in Urban Earthquake Disaster Mitigation

PEER Report 2001/16
Pacific Earthquake Engineering Research Center
College of Engineering
University of California, Berkeley

December 2001

ABSTRACT

Investigated in this report is the basic premise that the roof displacement of a multistory building can be determined from the deformation of an SDF system. For this purpose, the response of both systems is determined rigorously by nonlinear response history analysis, without introducing any of the approximations underlying the simplified methods for estimating the deformation of an SDF system (see, e.g., FEMA-273 or ATC-40 guidelines). The statistics of the SDF-system estimate of roof displacement are presented for a variety of building frames and six SAC buildings subjected to ground motion ensembles.

Two sets of structural systems and ground motions are considered. The first set is generic one-bay frames of six different heights: 3, 6, 9, 12, 15, and 18 stories designed for ductility factor $\mu = 1,\ 1.5,\ 2, 4, \text{and}\ 6$ subjected to 20 large-magnitude, small-distance records. The second set is six "SAC" buildings—9- and 20-story model buildings designed according to Los Angeles, Seattle, and Boston codes—subjected to 20 ground motion records representing 2% probability of exceedance in 50 years.

Presented are the statistics of two roof-displacement, u_r, ratios, $\left(u_r^*\right)_{\text{SDF}} = \left(u_r\right)_{\text{SDF}} \div \left(u_r\right)_{\text{NL-RHA}}$ and $\left(u_r^*\right)_{\text{MPA}} = \left(u_r\right)_{\text{MPA}} \div \left(u_r\right)_{\text{NL-RHA}}$, where the subscripts NL-RHA, MPA, and SDF denote the exact peak value determined by nonlinear RHA, approximate value from modal pushover analyses (MPA), and the SDF-system estimate. The data presented include histograms of the 20 values, range of values, median value, and dispersion measure.

These data for generic frames indicate that the first-"mode" SDF system overestimates the median roof displacement for systems subjected to large ductility demand μ, but underestimates for small μ, The bias and dispersion tend to increase for longer-period systems for every value of μ. Similar data for SAC buildings demonstrate that the bias and dispersion on the SDF estimate of roof displacement increases when P-delta effects (due to gravity loads) are included. The SDF estimate of roof displacement due to individual ground motions can be alarmingly small (as low as 0.312 to 0.817 of the "exact" value for the six SAC buildings) or surprisingly large (as large as 1.45 to 2.15 of the "exact" value for Seattle and Los Angeles buildings), especially when P-delta effects are included. The situation is worse than indicated by these data because they do not include several cases where the first-"mode" SDF system

collapsed but the building as a whole did not. This large discrepancy arises because for individual ground motions the SDF system may underestimate or overestimate the yielding-induced permanent drift in the "exact" response determined by nonlinear RHA.

While this discrepancy is not improved significantly by including higher "mode" contributions, the MPA procedure has the advantage of reducing the dispersion in the roof displacement and the underestimation of the median roof displacement for elastic or nearly elastic cases at the expense of increasing slightly the overestimate of roof displacement of buildings responding far into the inelastic range.

ACKNOWLEDGMENTS

This research investigation is funded by the National Science Foundation under Grant CMS-9812531, a part of the U.S.-Japan Cooperative Research in Urban Earthquake Disaster Mitigation. This financial support is gratefully acknowledged. The writers have benefited from discussions with Chris Poland, Jon Heintz, and Ken Yu of Degenkolb Engineers, and Helmut Krawinkler and C. Allin Cornell of Stanford University.

CONTENTS

LIST OF TABLES

LIST OF FIGURES

1 Introduction

It is now common in structural engineering practice to estimate seismic demands by the nonlinear static procedure (NSP) or pushover analysis detailed in FEMA-273 [1997] or ATC-40 guidelines [1996]. The seismic demands are computed by nonlinear static analysis of the structure subjected to monotonically increasing lateral forces with an invariant height-wise distribution until a target value of roof displacement is reached. This roof displacement value is determined from the earthquake-induced deformation of an inelastic SDF system derived from the pushover curve and has been compared with the "exact" value from nonlinear response history analysis (RHA) [Miranda, 1991; Collins, Wen, and Foutch, 1996; Gupta and Krawinkler, 2000].

Recently, much work has been done to develop and evaluate simplified methods for estimating the peak deformation of this inelastic SDF system, which has led to the capacity spectrum method detailed in ATC-40 and FEMA-274 [1997] reports, and the "coefficient method" in the FEMA-273 guidelines. The ATC-40 version of the capacity spectrum method has been shown to be unreliable and inaccurate [Chopra and Goel, 2000]. The well-established inelastic response (or design) spectrum [Veletsos and Newmark, 1960; Newmark and Hall, 1982] has been advocated as an alternative procedure [Bertero, 1995; Reinhorn, 1997; Fajfar, 1999] and implemented graphically as a capacity-demand diagram method [Chopra and Goel, 1999].

This work investigates the basic premise that the roof displacement of a multistory building can be determined from the deformation of an SDF system. For this purpose, the responses of both systems are determined rigorously by nonlinear response history analysis, without introducing any of the approximations underlying the aforementioned simplified methods. The statistics of the SDF-system estimate of roof displacement are presented for a variety of frame buildings and ground motion ensembles, and improved results are achieved by modal pushover analysis [Chopra and Goel, 2002].

2 Structural Systems, Ground Motions, and Response Statistics

2.1 STRUCTURAL SYSTEMS AND GROUND MOTIONS

Two sets of structural systems and ground motions are considered. The first set is generic one-bay frames of six different heights: 3, 6, 9, 12, 15, and 18 stories. The height-wise distribution of stiffness is defined to achieve equal drifts in all stories under the lateral forces specified in the International Building Code (IBC). Assuming that the second moment of cross-sectional area for each beam and its supporting columns in the story below are the same, numerical values for the flexural rigidities of structural elements were selected such that the fundamental vibration period is defined as $T_1 = 0.045H^{0.8}$, the mean-plus-one-standard deviation of measured periods [Goel and Chopra, 1997]. Frames with $T_1 = 0.028H^{0.8}$, the mean-minus-one-standard deviation of data, were also analyzed [Chintanapakdee and Chopra, 2002], but their results are not included here for brevity. The frames are designed according to the strong column-weak beam philosophy; therefore, plastic hinges form only at beam ends and the base of the first-story columns. Bending-moment yield strength distribution is designed such that yielding occurs simultaneously at all plastic hinges under the IBC lateral force distribution. The yield base shear is selected as $V_{by} = \left(A_y / g\right)W$, where W is the total weight of the frame and A_y is the median (over 20 ground motions) pseudo-acceleration for an SDF system with vibration period $T_n = T_1$ and a ductility factor $\mu =$ 1, 1.5, 2, 4, and 6; five different designs are considered for each frame height.

The seismic excitation for these generic frames is defined by a set of 20 large-magnitude-small-distance records (LMSR) listed in Chintanapakdee and Chopra [2002]. These ground motions were obtained from California earthquakes with magnitudes ranging from 6.6 to 6.9 recorded at distances of 13 km to 30 km.

The second set of structural systems will be referred to as "SAC" buildings. SAC commissioned three consulting firms to design 3-, 9-, and 20-story model buildings with symmetric plan according to the local code requirements of three cities: Los Angeles, Seattle, and Boston. Described in detail in Gupta and Krawinkler [1999], the structural systems of these model buildings consisted of perimeter steel moment-resisting frames (SMRF). The N-S perimeter frames of 9- and 20-story buildings are the second set of systems analyzed in this paper for two conditions: excluding or including P-delta effects due to gravity loads.

For all three locations, sets of 20 ground motion records were assembled representing probabilities of exceedance of 2% and 10% in 50 years (return periods of 2475 and 475 years, respectively) [Somerville, 1997]. The 2/50 set of records is used in the subsequent analysis.

2.2 RESPONSE STATISTICS

The dynamic response of each structural system to each of the 20 ground motions was determined by the three procedures described in the next section: nonlinear response history analysis (RHA), uncoupled modal response history analysis (UMRHA), and modal pushover analysis (MPA). Including only the first-mode contribution in the latter two approximate procedures provides the SDF-system estimate of response. The "exact" peak value of roof displacement, u_r, determined by nonlinear RHA is denoted by $(u_r)_{\text{NL-RHA}}$, the approximate value from MPA by $(u_r)_{\text{MPA}}$, and the SDF-system estimate by $(u_r)_{\text{SDF}}$. From these data for each ground motion, two displacement ratios are determined: $\left(u_r^*\right)_{\text{SDF}} = (u_r)_{\text{SDF}} \div (u_r)_{\text{NL-RHA}}$ and $\left(u_r^*\right)_{\text{MPA}} = (u_r)_{\text{MPA}} \div (u_r)_{\text{NL-RHA}}$. An approximate method is invariably biased in the sense that the median of the displacement ratio differs from one, underestimates the median response if the ratio is less than one, and provides an overestimate if the ratio exceeds one.

Presented in this paper are $n(=20)$ observed values, x_i of a displacement ratio in the form of a histogram, the median value, $\hat{x}$, defined as the geometric mean and the dispersion measure, δ, defined as

$$\hat{x} = \exp\left[\frac{\sum_{i=1}^{n} \ln x_i}{n}\right]; \qquad \delta = \left[\frac{\sum_{i=1}^{n} (\ln x_i - \ln \hat{x})^2}{n-1}\right]^{1/2} \tag{1}$$

For small values, e.g., 0.3 or less, the above dispersion measure is close to the coefficient of variation. In subsequent sections we will use loosely the term "dispersion" when referring to this measure. Equations (1a) and (1b) are logical estimators for the median and dispersion, especially if the data are sampled from lognormal distribution [Benjamin and Cornell, 1970], which is known to be appropriate for earthquake response of structures. In the case where one or more excitations caused collapse of the building or its first-mode system, the median and dispersion were estimated by a counting method. The 20 data values for a displacement ratio were sorted in ascending order, the median was estimated as the average of the 10^{th} and 11^{th} values starting from the lowest value; the 84^{th}-percentile value as the 17^{th} value; and the dispersion = log (84^{th} percentile value) – log (median value).

Before presenting such response data for inelastic response of the selected systems, we will consider their response assuming elastic behavior. In this case the nonlinear RHA procedure specializes to linear RHA and the MPA procedure to standard response spectrum analysis (RSA); thus, the latter displacement ratio is written as: $\left(u_r^*\right)_{\text{RSA}} = \left(u_r\right)_{\text{RSA}} \div \left(u_r\right)_{\text{RHA}}$.

3 Roof Displacement: Elastic Analysis Procedures

3.1 MODAL RESPONSE HISTORY ANALYSIS (RHA)

The differential equations governing the response of a multistory building to horizontal earthquake ground motion $\ddot{u}_g(t)$ are as follows:

$$\mathbf{m}\ddot{\mathbf{u}} + \mathbf{c}\dot{\mathbf{u}} + \mathbf{k}\mathbf{u} = -\mathbf{m}\boldsymbol{\iota}\,\ddot{u}_g(t) \tag{2a}$$

where $\mathbf{u}$ is the vector of N lateral floor displacements relative to the ground, $\mathbf{m}$, $\mathbf{c}$, and $\mathbf{k}$ are the mass, classical damping, and lateral stiffness matrices of the systems; each element of the influence vector $\boldsymbol{\iota}$ is equal to unity.

The right side of Eq. (2a) can be interpreted as effective earthquake forces:

$$\mathbf{p}_{\text{eff}}(t) = -\mathbf{m}\boldsymbol{\iota}\,\ddot{u}_g(t) \tag{2b}$$

The spatial distribution of these effective forces over the height of the building is defined by the vector $\mathbf{s} = \mathbf{m}\boldsymbol{\iota}$ and their time variation by $\ddot{u}_g(t)$. This force distribution can be expanded as a summation of modal inertia force distribution $\mathbf{s}_n$ [Chopra, 2001: Section 13.1.2]:

$$\mathbf{m}\boldsymbol{\iota} = \sum_{n=1}^{N} \mathbf{s}_n = \sum_{n=1}^{N} \Gamma_n \mathbf{m}\boldsymbol{\phi}_n \tag{3}$$

where $\boldsymbol{\phi}_n$ is the nth natural vibration mode of the structure, and

$$\Gamma_n = \frac{L_n}{M_n} \qquad L_n = \boldsymbol{\phi}_n^T \mathbf{m}\boldsymbol{\iota} \qquad M_n = \boldsymbol{\phi}_n^T \mathbf{m}\boldsymbol{\phi}_n \tag{4}$$

The effective earthquake forces can then be expressed as

$$\mathbf{p}_{\text{eff}}(t) = \sum_{n=1}^{N} \mathbf{p}_{\text{eff},n}(t) = \sum_{n=1}^{N} -\mathbf{s}_n \ddot{u}_g(t) \tag{5}$$

The contribution of the *n*th-mode to **s** and to $\mathbf{p}_{\text{eff}}(t)$ are

$$\mathbf{s}_n = \Gamma_n \mathbf{m}\boldsymbol{\phi}_n \qquad \mathbf{p}_{\text{eff},n}(t) = -\mathbf{s}_n \ddot{u}_g(t) \tag{6}$$

The response of the MDF systems to $\mathbf{p}_{\text{eff},n}(t)$ is entirely in the *n*th-mode, with no contributions from other modes. Therefore the floor displacements are

$$\mathbf{u}_n(t) = \boldsymbol{\phi}_n q_n(t) \tag{7}$$

where the modal coordinate $q_n(t)$ is governed by

$$\ddot{q}_n + 2\zeta_n \omega_n \dot{q}_n + \omega_n^2 q_n = -\Gamma_n \ddot{u}_g(t) \tag{8}$$

in which ω_n is the natural vibration frequency and ζ_n is the damping ratio for the *n*th-mode. The solution $q_n(t)$ of Eq. (8) is given by

$$q_n(t) = \Gamma_n D_n(t) \tag{9}$$

where $D_n(t)$ is governed by the equation of motion for the *n*th-mode linear SDF system, an SDF system with vibration properties—natural frequency ω_n and damping ratio ζ_n—of the *n*th-mode of the MDF system, subjected to $\ddot{u}_g(t)$:

$$\ddot{D}_n + 2\zeta_n \omega_n \dot{D}_n + \omega_n^2 D_n = -\ddot{u}_g(t) \tag{10}$$

Substituting Eq. (9) into Eq. (7) gives the floor displacements

$$\mathbf{u}_n(t) = \Gamma_n \boldsymbol{\phi}_n D_n(t) \tag{11}$$

In particular, the roof displacement is

$$u_{rn}(t) = \Gamma_n \boldsymbol{\phi}_{rn} D_n(t) \tag{12}$$

Equation (12) represents the response of the MDF system to $\mathbf{p}_{\text{eff},n}(t)$ [Eq. (6b)]. Therefore, the roof displacement due to the total excitation $\mathbf{p}_{\text{eff}}(t)$ is

$$u_r(t) = \sum_{n=1}^{N} u_{rn}(t) = \sum_{n=1}^{N} \Gamma_n \phi_{rn} D_n(t) \tag{13}$$

and its peak (or maximum absolute) value over time is denoted by $(u_r)_{\text{RHA}}$.

This is the classical modal RHA procedure: Eq. (8) is the standard modal equation governing $q_n(t)$, Eq. (12) defines the contribution of the *n*th-mode to the roof displacement, and Eq. (13) reflects combining the response contributions of all modes; however, these standard equations have been derived in an unconventional way. In contrast to the classical derivation found in textbooks [e.g., Chopra, 2001; Sections 12.4 and 13.1.3], we have used the modal expansion of the spatial distribution of the effective earthquake forces. This concept will provide a rational basis for investigating later the accuracy of an SDF system to estimate the target roof displacement for pushover analysis.

3.2 MODAL RESPONSE SPECTRUM ANALYSIS (RSA)

The peak value $(u_r)_{\text{RHA}}$ of the roof displacement can be estimated directly from the response spectrum for the ground motion without carrying out the RHA implied in Eqs. (8) through (13). In such an RSA, the peak value u_{rno} of the *nth*-mode contribution, $u_{rn}(t)$ to roof displacement $u_r(t)$ is determined from

$$u_{rno} = \Gamma_n \phi_{rn} D_n \tag{14}$$

where D_n is the peak value of deformation $D_n(t)$ of the *n*th-mode linear SDF system governed by Eq. (10) and the ordinate $D(T_n, \zeta_n)$ of the deformation response (or design) spectrum for the *n*th-mode SDF system; $T_n = 2\pi/\omega_n$ is the natural vibration period of the *n*th-mode of the MDF system.

For planar analysis of symmetric-plan buildings with well-separated frequencies, the peak modal responses are combined according to the SRSS rule to obtain an estimate of the total roof displacement:

$$(u_r)_{\text{RSA}} = \left(\sum_{n=1}^{N} u_{rno}^2 \right)^{1/2} \tag{15}$$

3.3 SDF-SYSTEM ESTIMATE

Considering only the first-mode response leads to an SDF-system estimate of the roof displacement, which is defined by Eq. (14), specialized for the first mode:

$$\left(u_r\right)_{\text{SDF}} = \Gamma_1 \phi_{r1} D_1 \tag{16}$$

4 Comparative Evaluation of Elastic Analysis Procedures

4.1 GENERIC FRAMES

Shown in Fig. 1 are the median and dispersion of the ratio $\left(u_r^*\right)_{\text{SDF}}$ for elastic frames plotted against the fundamental vibration period (or number of stories). This ratio starts very close to 1.0 for the 3-story frame and decreases to 0.85 for the 15-story frame, indicating that the SDF estimate, $\left(u_r\right)_{\text{SDF}}$, is biased in the sense that it underestimates the roof displacement and that this bias increases for taller (or longer-period) frames. The SDF system consistently underestimates the roof displacement because it ignores the higher mode contributions that are increasingly significant as the fundamental period lengthens [Chopra, 2001, Chapter 18]. For the same reasons, dispersion starts at close to zero for the 3-story frame and increases to 0.15 for the 18-story frame.

When higher-mode contributions are included in RSA, the median of the ratio $\left(u_r^*\right)_{\text{RSA}}$ becomes closer to 1.0 compared to $\left(u_r^*\right)_{\text{SDF}}$, indicating that the bias—although still an underestimation—has decreased (see Fig. 1). Because the peak modal response for each mode is computed exactly by RHA [Eq. (10)], the remaining bias is entirely due to approximations associated with the modal combination rule [Eq. (15)]. While this source of approximation is well known, it should be noted that the bias is consistently an underestimation. The dispersion of roof displacement is also reduced when higher mode contributions are included.

While the median and dispersion of the displacement ratio $\left(u_r^*\right)_{\text{SDF}}$ are two important sample statistics, data for individual ground motions are also of interest. For this purpose, histograms of the 20 values of the ratio are plotted in Fig. 2. Note that while the SDF-system provides an accurate estimate of displacement of the 3-story frame for every ground motion, it underestimates the displacement of the 6-story and taller frames for a large majority of excitations. This estimate can be alarmingly small for a few excitations. The smallest values of $\left(u_r^*\right)_{\text{SDF}}$ encountered are 0.96, 0.65, 0.62, 0.76, 0.70, and 0.57 for 3, 6, 9, 12, 15, and 18-story frames, respectively. As expected, when higher mode contributions are included, the histograms of the displacement ratio $\left(u_r^*\right)_{\text{RSA}}$ shift to larger values compared to $\left(u_r^*\right)_{\text{SDF}}$ and the range of values narrows for longer-period frames, however, not for shorter period frames (see Figs. 2 and 3).

To better understand the reasons for this large underestimation of roof displacement, Fig. 4 shows the time variation of roof displacement due to individual vibration modes, its total values [Eq. (13)], and the $\left(u_r\right)_{\text{RSA}}$ value [Eq. (15)] for the 6-story frame due to two of the 20 ground motions considered. Consistent with popular belief, the first mode for one of the excitations is dominant, therefore the SDF estimate, $\left(u_r\right)_{\text{SDF}}$, of roof displacement is essentially exact (4.71 cm versus 4.67 cm.). For the other excitation, however, while the displacement due to the first mode is largest among all modes, the relative contributions of various modes and how they combine is such that the exact peak response (5.23 cm) is much larger than the first mode value (3.41 cm); the SDF system underestimates the roof displacement by 35%. If the contributions of the first three modes are included in RSA, the error is reduced slightly and the roof displacement is underestimated by 26% (3.85 cm versus 5.23 cm).

4.2 SAC BUILDINGS

The earthquake response of each building to each SAC ground motion is computed under the assumption that the structure remains elastic. Table 1a shows the median and dispersion of the ratio $\left(u_r^*\right)_{\text{SDF}}$ for the six SAC buildings. The median ratio is less than 1.0, indicating that the

SDF-system estimate $(u_r)_{\text{SDF}}$ is biased toward underestimating the roof displacement because the higher mode contributions are ignored. The bias and dispersion varies among the three 9-story buildings (and the three 20-story buildings) because the significance of higher mode responses depends on their fundamental vibration period and on the frequency characteristics of different sets of ground motions for the three locations. For each location—with one exception—the bias and dispersion are smaller for the 9-story building because the fundamental mode contribution is more dominant in its roof displacement compared to the 20-story structure. As expected, when higher mode contributions are included according to RSA, the bias and dispersion decrease; the remaining bias is associated with the modal combination rule. As in the case of generic frames, the roof displacement is consistently underestimated, even if all significant modes are included.

The histograms of the 20 values of the displacement ratio $\left(u_r^*\right)_{\text{SDF}}$ for each of the six SAC buildings (Fig. 5) indicate that the SDF-system underestimates the roof displacement of 9-story buildings due to 19, 18, and 17 of the 20 ground motions for Boston, Seattle, and Los Angeles locations, respectively; for 20-story buildings it is underestimated by all excitations except one for the Boston structure. This estimate of roof displacement is surprisingly small for a few excitations. The roof displacement is underestimated by as much as 46%, 41%, and 40% for 9-story buildings in Boston, Seattle, and Los Angeles, and by 47%, 43%, and 39% for 20-story buildings in these three locations. As expected, when higher mode contributions are included, the histograms of the displacement ratio $\left(u_r^*\right)_{\text{RSA}}$ shift to larger values compared to $\left(u_r^*\right)_{\text{SDF}}$; furthermore, the range of values narrows for the Seattle and Los Angeles buildings, however, not for the Boston buildings (see Fig. 6).

To investigate this large underestimation of roof displacement, the response history of modal contributions and of the combined value of roof displacement for the 9-story Los Angeles building due to two of the 20 ground motions is presented in Fig. 7; also noted is the $(u_r)_{\text{RSA}}$ value from Eq. (15). Consistent with the prevailing view, the first mode for one of these excitations is strongly dominant; as shown in Fig. 7a, the SDF-system estimate of roof displacement is essentially exact (192 cm versus 191 cm). For another excitation, however, the SDF-system estimate (48.6 cm) is 40% less than the "exact" value (80.8 cm). If the contributions

of the first three modes are included in RSA, the underestimation is reduced to 28% (58.6 cm versus 80.8 cm).

5 Roof Displacement: Inelastic Analysis Procedures

5.1 NONLINEAR RESPONSE HISTORY ANALYSIS

The equations of motion for inelastic systems are a generalization of Eq. (2a):

$$\mathbf{m}\ddot{\mathbf{u}} + \mathbf{c}\dot{\mathbf{u}} + \mathbf{f}_s\left(\mathbf{u}, sign\,\dot{\mathbf{u}}\right) = -\mathbf{m}\boldsymbol{\iota}\,\ddot{u}_g\left(t\right) \tag{17}$$

where $\mathbf{f}_s\left(\mathbf{u}, sign\,\dot{\mathbf{u}}\right)$ denotes the hysteretic relations between lateral forces $\mathbf{f}_s$ at the N floor levels and lateral displacements $\mathbf{u}$. The standard approach is to solve directly these coupled equations, leading to the "exact" nonlinear RHA. The peak value of roof displacement determined by this procedure is denoted as $\left(u_r\right)_{\text{NL-RHA}}$.

Although classical modal analysis is not valid for inelastic systems, Eq. (17) will be transformed later to the modal coordinates of the corresponding linear system. Each structural element of this elastic system is defined as having the same stiffness as the initial stiffness of the structural element of the inelastic system. Both systems have the same mass and damping. Therefore, the natural vibration periods and modes of the corresponding linear system are the same as the vibration properties of the inelastic system undergoing small oscillations (within the linear range).

Expanding the displacements of the inelastic system in terms of the natural vibration modes of the corresponding linear system we get

$$\mathbf{u}\left(t\right) = \sum_{n=1}^{N} \boldsymbol{\phi}_n q_n\left(t\right) \tag{18}$$

Substituting Eq. (18) in Eq. (17), premultiplying by $\boldsymbol{\phi}_n^T$, and using the mass- and classical damping-orthogonality property of modes gives

$$\ddot{q}_n + 2\zeta_n \omega_n \dot{q}_n + \frac{F_{sn}}{M_n} = -\Gamma_n \ddot{u}_g(t) \qquad n = 1, 2, \ldots N \tag{19}$$

where the only term that differs from Eq. (8) involves

$$F_{sn} = F_{sn}(\mathbf{q}, sign\,\dot{\mathbf{q}}) = \boldsymbol{\phi}_n^T \mathbf{f}_s(\mathbf{u}, sign\,\dot{\mathbf{u}}) \tag{20}$$

This resisting force depends on all modal coordinates $q_n(t)$, implying coupling of modal coordinates because of yielding of the structure.

Equation (19) represents N equations in the modal coordinates q_n. Unlike Eq. (8) for linearly elastic systems, these equations are coupled for inelastic systems. In principle, solving these coupled equations simultaneously and using Eq. (18) will give the same results for roof displacement as obtained directly from Eq. (17); however, Eq. (19) is rarely used because it offers no particular advantage over Eq. (17).

5.2 UNCOUPLED MODAL RESPONSE HISTORY ANALYSIS (UMRHA)

Neglecting the coupling of the N equations in modal coordinates [Eq. (19)] leads to the uncoupled modal response history analysis (UMRHA) procedure. This approximate RHA procedure facilitates investigating the SDF-system estimate of roof displacement of inelastic MDF systems.

The spatial distribution $\mathbf{s}$ of the effective earthquake forces is expanded into the modal contributions $\mathbf{s}_n$ according to Eq. (3), where $\boldsymbol{\phi}_n$ are now the modes of the corresponding linear system. The equations governing the response of the inelastic system to $\mathbf{p}_{\text{eff},n}(t)$ given by Eq. (6b) are

$$\mathbf{m}\ddot{\mathbf{u}} + \mathbf{c}\dot{\mathbf{u}} + \mathbf{f}_s(\mathbf{u}, sign\,\dot{\mathbf{u}}) = -\mathbf{s}_n \ddot{u}_g(t) \tag{21}$$

The solution of Eq. (21) for inelastic systems will no longer be described by Eq. (7) because "modes" other than the nth-"mode" will also contribute to the solution; however, the nth-"mode" is dominant even for inelastic systems [Chopra and Goel, 2002].

Approximating the response of the structure to excitation $\mathbf{p}_{\text{eff},n}(t)$ by Eq. (7), substituting Eq. (7) in Eq. (19), and premultiplying by $\boldsymbol{\phi}_n^T$ gives Eq. (20) except for the important approximation that F_{sn} now depends only on one modal coordinate, q_n:

$$F_{sn} = F_{sn}\left(q_n, sign\ \dot{q}_n\right) = \boldsymbol{\phi}_n^T \mathbf{f}_s\left(q_n, sign\ \dot{q}_n\right) \tag{22}$$

With this approximation, the solution of Eq. (19) can be expressed by Eq. (9), where $D_n(t)$ is governed by

$$\ddot{D}_n + 2\zeta_n \omega_n \dot{D}_n + \frac{F_{sn}}{L_n} = -\ddot{u}_g(t) \tag{23}$$

and

$$F_{sn} = F_{sn}\left(D_n, sign\ \dot{D}_n\right) = \boldsymbol{\phi}_n^T \mathbf{f}_s\left(D_n, sign\ \dot{D}_n\right) \tag{24}$$

is related to $F_{sn}\left(q_n, sign\ \dot{q}_n\right)$ because of Eq. (9).

Equation (23) may be interpreted as the governing equation for the *n*th-"mode" inelastic SDF system, an SDF system with (1) small amplitude vibration properties—natural frequency ω_n and damping ratio ζ_n—of the *n*th-mode of the corresponding linear MDF system; and (2) $F_{sn}/L_n - D_n$ relation between resisting force F_{sn}/L_n and modal coordinate D_n defined by Eq. (24). Solution of the nonlinear Eq. (23) formulated in this manner provides $D_n(t)$, which substituted into Eq. (11) gives the floor displacements of the structure associated with the *n*th-"mode" inelastic SDF system. In particular, the roof displacement is given by Eq. (12), which now represents the roof displacement of the inelastic MDF system to $\mathbf{p}_{\text{eff},n}(t)$, the *n*th-mode contribution to $\mathbf{p}_{\text{eff},n}(t)$. Therefore the roof displacement due to the total excitation $\mathbf{p}_{\text{eff},n}(t)$ is given by Eq. (13). This is the UMRHA procedure, which for linear systems is identical to the classical modal RHA described in Section 3.1.

5.2.1 Properties of the *n*th-"Mode" Inelastic SDF System

To determine the $F_{sn}/L_n - D_n$ relation in Eq. (23), the relationship between lateral forces $\mathbf{f}_s$ and D_n in Eq. (22) should be determined by nonlinear static analysis of the structure as the structure

undergoes displacements $\mathbf{u} = D_n \boldsymbol{\phi}_n$ with increasing D_n. However, most commercially available software cannot implement such displacement-controlled analysis. An alternative approach, which is an approximation, is to conduct a force-controlled nonlinear static analysis of the structure subjected to lateral forces distributed over the building height according to

$$\mathbf{s}_n^* = \mathbf{m}\boldsymbol{\phi}_n \tag{25}$$

Such nonlinear static analysis provides the so-called pushover curve, which is a plot of base shear V_{bn} against roof displacement u_{rn}. A bilinear idealization of this pushover curve for the *n*th-"mode" is shown in Fig. 8. At the yield point, the base shear is V_{bny} and roof displacement is u_{rny}. P-delta effects arising from gravity loads are included in the pushover curve for the first mode but not for other modes.

This pushover curve is converted to the desired $F_{sn}/L_n - D_n$ relation shown in Fig. 8b, where the yield values of F_{sn}/L_n and D_n are

$$\frac{F_{sny}}{L_n} = \frac{V_{bny}}{M_n^*} \qquad D_{ny} = \frac{u_{rny}}{\Gamma_n \phi_{rn}} \tag{26}$$

in which $M_n^* = L_n \Gamma_n$ is the effective modal mass [Chopra, 2001, Section 13.2.5]. The two are related through

$$\frac{F_{sny}}{L_n} = \omega_n^2 D_{ny} \tag{27}$$

implying that the initial slope of the bilinear curve in Fig. 8b is ω_n^2. Knowing F_{sny}/L_n and D_{ny} from Eq. (26), the elastic vibration period T_n of the *n*th-"mode" inelastic SDF system is computed from

$$T_n = 2\pi \left(\frac{L_n D_{ny}}{F_{sny}} \right)^{1/2} \tag{28}$$

This value of T_n, which may differ from the period of the corresponding linear system, should be used in Eq. (23).

5.2.2 Underlying Assumptions and Accuracy

The UMRHA procedure is based on two principal assumptions and approximations: (1) the coupling between modal coordinates $q_n(t)$ arising from yielding of the system [recall Eqs. (19) and (20)] is neglected; and (2) the superposition of responses to $\mathbf{p}_{\text{eff},n}(t)$ $(n = 1, 2 \ldots N)$ according to Eq. (13) is strictly valid only for linearly elastic systems and is only approximate for inelastic systems. Secondarily, the $F_{sn}/L_n - D_n$ relation is approximated by a bilinear curve to facilitate solution of Eq. (24) in UMRHA.

While the coupled nonlinear equation [Eq. (21)] must be solved to determine the "exact" roof displacement due to $\mathbf{p}_{\text{eff},n}(t)$, the first assumption implies that an approximate result can be obtained from Eq. (12), with $D_n(t)$ determined by nonlinear RHA of the *n*th-mode inelastic SDF system governed by Eq. (23). Figure 9 compares this approximate solution for a 6-story frame with SDF-system $\mu = 6$ and two ground motions with the "exact" result for $n = 1, 2,$ and 3 in Fig. 9. Errors in this SDF-system method are only a few percent, although the frame deforms well into the inelastic range and undergoes considerable permanent drift. This demonstrated accuracy of an SDF-system method to estimate the response to $\mathbf{p}_{\text{eff},n}(t)$ has been confirmed for buildings ranging from 3 to 18 stories, SDF-system ductility varying from 1 to 6, and 20 ground motions.

The second assumption implies that superposition [Eq. (13)] of the "exact" roof displacements $u_{rn}(t)$ due to $\mathbf{p}_{\text{eff},n}(t)$—$n$ = 1, 2, 3…—determined by nonlinear RHA of the MDF system [Eq. (21)]—will provide a good approximation to the "exact" response of the MDF system to $\mathbf{p}_{\text{eff}}(t)$ ([Eq. (2)]. Based on Fig. 9, this implies that the superposition of the approximate $u_{rn}(t)$ determined using $D_n(t)$ of the *n*th-mode inelastic SDF system should provide a good approximation to the "exact" value; however, as demonstrated later, this is not always the case.

5.3 MODAL PUSHOVER ANALYSIS

The peak value u_{rno} of $u_{rn}(t)$, the roof displacement of the inelastic MDF system due to earthquake forces $\mathbf{p}_{\text{eff},n}(t)$, can be estimated from Eq. (14) where D_n is now the peak value of deformation $D_n(t)$ of the *n*th-mode inelastic SDF system. It can be determined by solving Eq. (24) or from the inelastic response (or design spectrum) [Chopra, 2001; Sections 7.6 and 7.12]. As shown earlier for elastic systems [Chopra and Goel, 2002], u_{rno} also represents the exact peak value of the *n*th-mode contributions $u_{rn}(t)$ to $u_r(t)$. Thus, we will refer to u_{rno} as the peak "modal" response even in the case of inelastic systems.

The peak modal responses, u_{rno}, each determined by pushover analysis for force distribution $\mathbf{s}_n^*$ and dynamic analysis of the *n*th-mode inelastic SDF system, may be combined using an appropriate modal combination rule [e.g., Eq. (15)]—although it is strictly valid only for elastic response—to obtain an MPA-estimate of the total roof displacement:

$$(u_r)_{\text{MPA}} = \left(\sum_{n=1}^{N} u_{rno}^2 \right)^{1/2} \tag{29}$$

The MPA procedure when applied to linear systems is equivalent to the standard RSA procedure of Section 3.2 [Chopra and Goel, 2002].

5.4 SDF-SYSTEM ESTIMATE

In current nonlinear static (or pushover) analysis procedures, only the first term is retained in Eq. (29) and it is obtained for an SDF system determined from static analysis of the structure subjected to lateral-force distributions specified in the FEMA-273 guidelines instead of the distribution defined by Eq. (25). Considering only the first-"mode" contribution leads to an SDF-system estimate of the roof displacement, which is given by Eq. (16), where D_1 is now the peak deformation of the first-"mode" inelastic SDF system.

6 Comparative Evaluation of Inelastic Analysis Procedures

6.1 GENERIC FRAMES

The median and dispersion of the ratio $\left(u_r^*\right)_{\text{SDF}}$ are plotted versus the fundamental vibration period (or number of stories) in Figs. 10a-b and versus the design ductility factor, μ, in Figs. 11a-b. This median ratio starts very close to 1.0 for 3-story frames irrespective of the design ductility factor, μ, but increasingly differs from 1.0 and becomes increasingly dependent on μ as T_1 becomes longer (see Figs. 10a and 11a). The SDF-system estimate, $\left(u_r\right)_{\text{SDF}}$, is biased as expected, but the nature and magnitude of this bias depends on μ. For smaller μ, the SDF-system method underestimates the roof displacement; this bias increases for longer-period systems (or taller frames) just as in the case of elastic systems (Fig. 1). The situation is reversed for larger μ; for $\mu = 6$ the SDF-system method overestimates the roof displacement, and this bias increases for taller frames (Figs. 10a and 11a). For intermediate values of μ, the ratio $\left(u_r^*\right)_{\text{SDF}}$ is closer to one, implying that the SDF-system estimate of roof displacement is relatively more accurate for frames of all heights. The dispersion tends to increase for taller frames for every value of μ (Fig. 10b). It is smallest for elastic systems and tends to increase with the design ductility factor, but this trend is not perfect (see Fig. 11b).

Including higher "mode" contributions according to the MPA procedure obviously increases the estimate $\left(u_r\right)_{\text{MPA}}$ of the roof displacement relative to the SDF-system estimate

$(u_r)_{\text{SDF}}$, thus the $\left(u_r^*\right)_{\text{MPA}}$ plot is shifted up (compare Figs. 10a and 10c). As a result, MPA overestimates the roof displacement except for elastic or nearly elastic cases where it underestimates to a lesser degree than the SDF-system estimate. Generally, this overestimation is modest, except for combinations of very long periods and large design ductility values. Including higher "mode" contributions to the roof displacement reduces significantly the dispersion for lower values of μ and, to a lesser degree, for larger values of μ.

Shown in Fig. 12 are the histograms of the 20 values of the ratio $\left(u_r^*\right)_{\text{SDF}}$ together with the range of values and median value of this ratio for each of the six frames with design ductility factor $\mu = 6$. The SDF-system estimate of roof displacement can be alarmingly small for individual ground motions for frames as low as 6 stories and, of course, for taller frames. The smallest values of $\left(u_r^*\right)_{\text{SDF}}$ encountered are 0.89, 0.72, 0.73, 0.66, 0.72, and 0.75 for 3, 6, 9, 12, 15, and 18 story-frames, respectively. The SDF-system estimate can also be surprisingly large for a few excitations, especially for taller frames. The largest values of $\left(u_r^*\right)_{\text{SDF}}$ observed are 1.40, 1.62, 1.46, 1.38, 1.58 and 1.88 for 3, 6, 9, 12, 15, and 18-story frames. A comparison of Figs. 2 and 12 indicates that the $\left(u_r^*\right)_{\text{SDF}}$ ratio varies over a much wider range for inelastic systems—and good accuracy occurs less often—compared to elastic systems. The histograms of ratio $\left(u_r^*\right)_{\text{MPA}}$ shown in Fig. 13 demonstrate that the range of values does not narrow significantly, implying that even when higher "mode" contributions are included large error can occur in roof displacement estimates for individual ground motions.

To investigate the large error in the SDF-system estimate of roof displacement, the response history of "modal" contributions, the combined value determined by UMRHA, and the "exact" response by nonlinear RHA are presented for the 6-story frame designed for $\mu = 6$ due to three of the 20 ground motions in Figs. 14a-14c, respectively; also included is the $(u_r)_{\text{MPA}}$ value determined from Eq. (29). In the first case the first-"mode" contribution is dominant; yielding causes very little drift of the first-mode SDF system away from its zero-displacement position in spite of the large design ductility, and the SDF-system estimate of the roof

displacement is very close to the "exact" value determined by nonlinear RHA (see Fig. 14a). In the second case the first-"mode" contribution is dominant, but the yielding-induced permanent drift is much smaller than seen in the "exact" response by nonlinear RHA (see Fig. 14b). Consequently, the SDF system underestimates the roof displacement by 28%. In the third case the first-"mode" contribution remains dominant, but the yielding-induced permanent drift in the first-"mode" SDF system is larger than seen in the results of nonlinear RHA (Fig. 14c). Consequently, the SDF system overestimates the roof displacement by 62%.

For the latter two ground motions, little if any improvement is achieved by including higher "mode" contributions according to the UMRHA procedure. This persistent discrepancy implies that the second assumption identified earlier in developing the UMRHA procedure is not always valid; it works in Fig. 14a but not in Figs. 14b or 14c. When it does not work, the roof displacement $(u_r)_{\text{MPA}}$ estimated by MPA is also inaccurate (see values noted in Fig. 14). In principle, this estimate should be less accurate than the UMRHA result because it contains additional modal combination errors; however, that is not always the case because errors due to various approximations can cancel or reinforce each other.

6.2 SAC BUILDINGS

To facilitate interpretation of subsequent results, Fig. 15 shows the first-"mode" pushover curves for the six SAC buildings for two cases: P-delta effects due to gravity loads excluded or included, with the peak displacement identified for each of the 20 ground motions except for those excitations that caused collapse of the system. In the presence of P-delta effects, the number of excitations that caused collapse of the first-"mode" SDF systems is one for the Seattle 9-story building, three for the Los Angeles 9-story building, and six for the Los Angeles 20-story building. For these buildings the statistics of displacement ratios $\left(u_r^*\right)_{\text{SDF}}$ and $\left(u_r^*\right)_{\text{MPA}}$ were calculated by the counting method described in Section 2.2. Note that nonlinear RHA of these buildings and ground motions predicted a finite value of displacement and did not predict their collapse except for the Los Angeles 20-story building due to one ground motion.

Shown in Table 2 are the median and dispersion of the ratio $\left(u_r^*\right)_{\text{SDF}}$ for six SAC buildings for two cases: P-delta effects excluded or included. When these effects are excluded,

the SDF-system estimate of roof displacement has small bias for Seattle buildings, overestimates by 6% and 11% for Los Angeles 9- and 20-story buildings, and underestimates by 17% and 22% for Boston 9- and 20-story buildings, respectively. The dispersion is similar for all cases except that it is much smaller for the Los Angeles 20-story building, which is surprising because this building is driven well into the inelastic range (see Fig. 15f).

As shown in Table 2, when P-delta effects are included in both analyses—nonlinear RHA and first-"mode" SDF system—the bias in the SDF-system estimate of roof displacement is essentially unaffected for Boston buildings because they respond within their elastic range (see Figs. 15a-b) and for the Seattle 20-story building because only a few of the 20 ground motions excited it slightly beyond yield displacement (Fig. 15d). However, P-delta effects significantly influence the response of the other three buildings because most of the 20 ground motions excite them well beyond the yield displacement into the region of negative stiffness (see Figs. 15c, e, and f) and collapse occurs in some cases. This influence is apparent by the increased bias and dispersion of the SDF-system estimate of displacement (see Table 2).

Including higher mode contributions according to the MPA procedure obviously gives a larger roof displacement than the SDF-system estimate, thus the median $\left(u_r^*\right)_{\text{MPA}}$ values shown in Table 3 are larger compared to $\left(u_r^*\right)_{\text{SDF}}$ values shown in Table 2. The roof displacement, excluding P-delta effects, is now quite accurate; it is underestimated by only 5% for Boston buildings, overestimated by 5% or 7% for Seattle buildings, and 8% or 17% for Los Angeles buildings. Not only is the median value estimated more accurately by MPA, the dispersion is reduced for most cases.

As shown in Table 3 with P-delta effects included in nonlinear RHA and MPA, the MPA procedure estimates the median displacement almost perfectly for the Boston 9-story building, within 5% for the Seattle buildings, and overestimates it 21% or 27% for the Los Angeles buildings. Only for the Boston 20-story building does the procedure underestimate the displacement significantly—by 12%. P-delta effects increase the dispersion of the MPA estimate for roof displacement for all buildings, with significant increases in four cases. [The dispersion of the Los Angeles 20-story building could not be calculated because the 17$^{\text{th}}$ value (or 84$^{\text{th}}$ percentile value) required was not available; in this case, more than three excitations caused collapsed of the SDF system.]

Figures 16 and 17 show the histograms of the 20 values of the displacement ratio $\left(u_r^*\right)_{\text{SDF}}$ together with the range of values and the median values of this ratio for each of the six SAC buildings for two cases: P-delta effects excluded or included. For Los Angeles buildings, which are driven well into the inelastic range, this ratio is larger than one for many excitations, a result consistent with generic frames designed for a large ductility factor, μ. For Boston buildings, which remain close to elastic, $\left(u_r^*\right)_{\text{SDF}}$ is smaller than one for most ground motions, similar to the observation based on earlier elastic analyses (Fig. 5).

If we compare Figs. 16 and 17, note that the range of values for $\left(u_r^*\right)_{\text{SDF}}$ becomes much wider when P-delta effects due to gravity loads are included, implying that the SDF-system estimate of the roof displacement may now be considerably less accurate for individual ground motions. Clearly, the SDF-system estimate can be alarmingly small (as low as 0.312 to 0.817 for the six buildings) or surprisingly large (as large as 1.45 to 2.15 for Seattle and Los Angeles buildings) for individual ground motions, especially when P-delta effects are included. This situation is worse than indicated by Fig. 17 because it does not include several cases mentioned earlier where the first-"mode" SDF system collapsed, whereas the building as a whole did not. The SDF system overestimates the roof displacement of 9-story buildings due to seven and twelve ground motions for Seattle and Los Angeles locations, respectively, and of 20-story buildings due to eight excitations for the Seattle structure and eleven for the Los Angeles structure. The histograms of the ratio $\left(u_r^*\right)_{\text{MPA}}$ shown in Figs. 18 and 19 demonstrate that the range of values does not narrow for most buildings, implying that the error in estimating roof displacements due to individual ground motions can be considerable even when higher "mode" contributions are included.

To investigate the large discrepancy in the SDF-system estimate of roof displacement, the response history of "modal" contributions, the combined response determined by UMRHA, and the "exact" response from nonlinear RHA are presented for the Los Angeles 9-story building due to three of the 20 ground motions in Figs. 20a, 20b, and 20c, respectively, also included is the $\left(u_r\right)_{\text{MPA}}$ value determined from Eq. (29). In the first case the first-"mode" contribution is dominant; the peak response occurs at the end of the first large inelastic excursion before the

yielding-induced drift away from the zero-displacement position takes place, and the SDF-system estimate is highly accurate (see Fig. 20a). In the second case the first-"mode" contribution is dominant, but its permanent drift is much smaller than in the "exact" response determined by nonlinear RHA (see Fig. 20b), and the SDF-system method underestimates the roof displacement by 37%. Including the higher mode contributions in MPA improves the estimate only slightly. In the third case the first-"mode" contribution is dominant, but its permanent drift is much larger than in the "exact" response by nonlinear RHA (see Fig. 20c). Consequently, the SDF-system method overestimates the roof displacement by 65%. Including the higher mode contributions in MPA worsens the overestimation to 71%.

7 Implications for FEMA Pushover Analyses

The SDF system was derived herein from the pushover curve using the lateral force distribution associated with the fundamental vibration mode of the corresponding linear system [Eq. (25)]. However, the force distributions defined in FEMA-273 are different:

1. "Uniform" distribution: $s_j^* = m_j$ (where the floor number $j = 1, 2 \ldots N$);

2. Equivalent lateral force (ELF) distribution: $s_j^* = m_j h_j^k$ where h_j is the height of the *j*th floor above the base, and the exponent $k = 1$ for fundamental period $T_1 \le 0.5 \sec$, $k = 2$ for $T_1 \ge 2.5 \sec$; and varies linearly in between; and

3. SRSS distribution: $\mathbf{s}^*$ is defined by the lateral forces back-calculated from the story shears determined by response spectrum analysis of the structure, assumed to be linearly elastic.

Are the results presented earlier in this paper relevant to the FEMA-273 force distributions? To answer this question, Fig. 21a compares the pushover curves for the Los Angeles 9-story building associated with these force distributions together with the first-"mode" result; Fig. 21b shows the peak deformations of the SDF systems associated with three FEMA force distributions, plotted against the value from the first-"mode" inelastic SDF system. All these pushover curves and the deformations of the various SDF systems are similar. Thus the general observations concerning the SDF-system estimate of roof displacement presented earlier are valid for the FEMA-273 force distributions.

8 Conclusions

Elastic Buildings

1. When compared to "exact" values obtained from rigorous nonlinear RHA, the first-mode SDF system underestimates the median value of roof displacement over an ensemble of ground motions. The bias and dispersion of the displacement ratio $\left(u_r^*\right)_{\text{SDF}}$ increases for longer-period frames, median values as low as 0.850 for generic frames, and 0.741 for SAC buildings were observed, implying that the SDF-system underestimates roof displacement by 15% and 26%, respectively. The SDF-system estimate of roof displacement due to individual excitations can be alarmingly inaccurate.
2. When higher mode contributions to response are included in RSA, the bias and dispersion of the displacement ratio $\left(u_r^*\right)_{\text{RSA}}$ reduces; the remaining bias and dispersion is due to approximations associated with modal combination rules.

Inelastic Buildings

1. The first-"mode" SDF system estimate of the median roof displacement is biased, as expected, but the nature and magnitude of this bias depends on how far the structure is driven into the inelastic range, characterized by an overall ductility demand μ, For larger μ, the SDF-system method overestimates the median roof displacement, and this bias

increases for longer-period systems. The situation is reversed for small μ; the SDF-system method underestimates roof displacement, and this bias increases for longer-period systems.

2. The median values of $\left(u_r^*\right)_{\text{SDF}}$ ranged from 0.85 for 1.19 for generic frames, from 0.78 to 1.11 for SAC buildings without P-delta effects due to gravity loads, implying an underestimation by 22% to an overestimation by 11%, respectively.

3. The dispersion of the displacement ratio $\left(u_r^*\right)_{\text{SDF}}$ tends to increase for taller frames for every value of μ.

4. The bias and dispersion in the SDF estimate of roof displacement increases when P-delta effects (due to gravity loads) are included.

5. The SDF estimate of roof displacement due to individual ground motions can be alarmingly small (as low as 0.312 to 0.817 of the "exact" value for the six SAC buildings) or surprisingly large (as large as 1.45 to 2.15 of the "exact" value for Seattle and Los Angeles buildings), especially when P-delta effects are included. The situation is worse than indicated by these data because they do not include several cases where the first-"mode" SDF system collapsed whereas the building as a whole did not.

6. This large discrepancy arises because for individual ground motions the SDF system may underestimate or overestimate the yielding-induced permanent drift in the "exact" response determined by nonlinear RHA.

7. While this discrepancy is not improved significantly by including higher "mode" contributions, the MPA procedure has the advantage of reducing the dispersion in the roof displacement and the underestimation of the median roof displacement for elastic or nearly elastic cases at the expense of increasing slightly the overestimate of roof displacement of buildings responding far into the inelastic range.

References

Benjamin, J. R., and Cornell, C. Allin (1970). *Probability, statistics, and decision for civil engineers*. New York: McGraw-Hill.

Bertero, V. V. (1995). Tri-service manual methods. In *Performance-based seismic engineering of buildings*, ed. J. Soulages. Vision 2000. Sacramento, Calif.: Structural Engineers Assn. of California.

Building Seismic Safety Council (1997). *NEHRP guidelines for the seismic rehabilitation of buildings*, *FEMA-273*, *and Commentary, FEMA-274.* Washington, D.C.: Federal Emergency Management Agency.

Chintanapakdee, C., and Chopra, A. K. (2002). *Evaluation of modal pushover analyses for generic frames.* (Berkeley, Calif.: Pacific Earthq. Engrg. Res. Cen, Univ. of Calif., forthcoming.)

Chopra, A. K., and Goel, R. K. (1999). Capacity-demand-diagram methods based on inelastic design spectrum. *Earthq. Spectra* 15(4):637–56.

Chopra, A. K., and Goel, R. K. (2000). Evaluation of NSP to estimate seismic deformation: SDF systems. *J. Struc. Engrg.* 126(4):482–90. ASCE.

Chopra, A. K. (2001). *Dynamics of structures: Theory and applications to earthquake engineering*, 2d ed. Englewood Cliffs, N.J.: Prentice Hall.

Chopra, A. K., and Goel, R. K. (2002). A modal pushover analysis procedure for estimating seismic demands for buildings. *Earthq. Engrg. Struc. Dyn*. 31(3):561–82.

Collins, K. R., Wen, Y. K., and Foutch, D. A. (1996). Dual-level seismic design: a reliability-based methodology, *Earthq. Engrg. Struc. Dyn*., 25(12):1433–67.

Comartin, C. D., Niewiarowski, R. W., and Rojahn, C. Applied Technology Council (1996). *Seismic evaluation and retrofit of concrete buildings.* Report No. SSC 96-01, ATC-40. [Sacramento, Calif.]: Seismic Safety Commission, State of Calif.

Fajfar, P. (1999). Capacity spectrum method based on inelastic spectra. *Earthq. Engrg. Struc. Dyn*. 28(9):979–93.

Goel, R. K., and Chopra, A. K. (1997). Period formulas for moment-resisting frame buildings. *J. Struc. Engrg.* 123(11):1454–61. ASCE.

Gupta, A., and Krawinkler, H. (1999). *Seismic demands for performance evaluation of steel moment resisting frame structures (SAC Task 5.4.3).* Report No. 132. Stanford, Calif.: John A. Blume Earthq. Engrg. Cen., Stanford Univ.

Gupta, A., and Krawinkler, H. (2000). Estimation of seismic drift demand for frame structures, *Earthq. Engrg. Struc. Dyn*., 29(9):1287–1305.

Miranda, E. (1991). *Evaluation and upgrading of existing buildings*, Ph.D. Dissertation, Dept. of Civil Engrg., Univ. of Calif., Berkeley, Calif.

Newmark, N. M., and Hall, W. J. (1982). *Earthquake spectra and design.* Engineering monographs on earthquake criteria, structural design, and strong motion records, vol. 3*,* pp. 29–37. Berkeley, Calif.: Earthq. Engrg. Res. Inst.

Reinhorn, A. M. (1997). Inelastic analysis techniques in seismic evaluations, eds. P. Fajfar and H. Krawinkler. In *Seismic design methodologies for the next generation of codes,* pp. 277–87. Rotterdam: Balkema.

Somerville, P., Smith, N., Punyamurthula, S., and Sun, J. (1997). *Development of ground motion time histories for phase 2 of the FEMA/SAC steel project.* SAC Background document report No. SAC/BD-9/04. Sacramento, Calif.: SAC Joint Venture, 555 University Ave.

Veletsos, A. S., and Newmark, N. M. (1960). Effect of inelastic behavior on the response of simple systems to earthquake motions. In *Proc., 2nd World Conf. Earthq. Engrg,* vol. 2, pp. 895–912, Tokyo, Japan. Tokyo: Oh-Okayama, Meguro-Ku.

Table 1: **Median and dispersion of $\left(u_r^*\right)_{\text{SDF}}$ and $\left(u_r^*\right)_{\text{RSA}}$ for SAC buildings analyzed as elastic systems.**

Building	T_1 (sec)	$\left(u_r^*\right)_{\text{SDF}}$		$\left(u_r^*\right)_{\text{RSA}}$	
		Median	Dispersion	Median	Dispersion
Boston 9-Story	3.11	0.829	0.147	0.949	0.142
Boston 20-Story	3.11	0.783	0.184	0.956	0.135
Seattle 9-Story	2.99	0.821	0.160	0.912	0.0955
Seattle 20-Story	3.76	0.741	0.165	0.868	0.0857
Los Angeles 9-Story	2.27	0.912	0.128	0.944	0.0945
Los Angeles 20-Story	3.81	0.881	0.110	0.930	0.0697

Table 2: Median and dispersion of $\left(u_r^*\right)_{\text{SDF}}$ for SAC buildings.

Building	Gravity Loads Excluded		Gravity Loads Included	
	Median	Dispersion	Median	Dispersion
Boston 9-Story	0.830	0.152	0.860	0.177
Boston 20-Story	0.782	0.192	0.721	0.244
Seattle 9-Story	1.01	0.194	0.944[1]	0.411[1]
Seattle 20-Story	0.949	0.188	0.947	0.208
Los Angeles 9-Story	1.06	0.194	1.19[2]	0.331[2]
Los Angeles 20-Story	1.11	0.109	1.19[3]	N/A[3,4]

[1,2,3]Data for excitations that caused collapse of the SDF system are excluded, reducing the number of data to (1) 19, (2) 17, and (3) 14; the median and dispersion values are computed by the counting method.
[4]Dispersion could not be calculated because the 17th value (or the 84th percentile value) required was not available; in this case, more than 3 excitations caused collapse of the SDF system.

Table 3: Median and dispersion of $\left(u_r^*\right)_{\text{MPA}}$ for SAC buildings.

Building	Gravity Loads Excluded		Gravity Loads Included	
	Median	Dispersion	Median	Dispersion
Boston 9-Story	0.951	0.148	0.995	0.159
Boston 20-Story	0.954	0.141	0.881	0.224
Seattle 9-Story	1.07	0.191	0.990[1]	0.379[1]
Seattle 20-Story	1.05	0.210	1.05	0.212
Los Angeles 9-Story	1.08	0.184	1.21[2]	0.343[2]
Los Angeles 20-Story	1.17	0.100	1.27[3]	N/A[3,4]

[1,2,3]Data for excitations that caused collapse of the SDF system are excluded, reducing the number of data to (1) 19, (2) 17, and (3) 14; the median and dispersion values are computed by the counting method.
[4]Dispersion could not be calculated because the 17th value (or the 84th percentile value) required was not available; in this case, more than 3 excitations caused collapse of the SDF system.

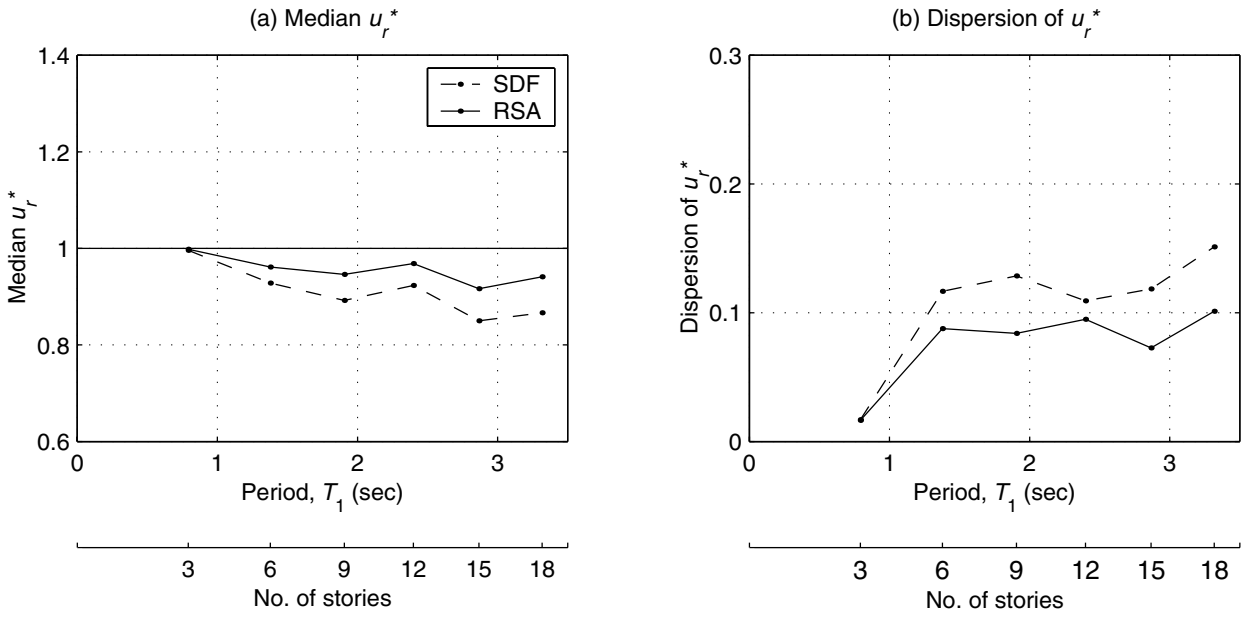

Fig. 1: **Median and dispersion of $\left(u_r^*\right)_{\text{SDF}}$ and $\left(u_r^*\right)_{\text{RSA}}$ versus fundamental vibration period T_1 for generic elastic frames.**

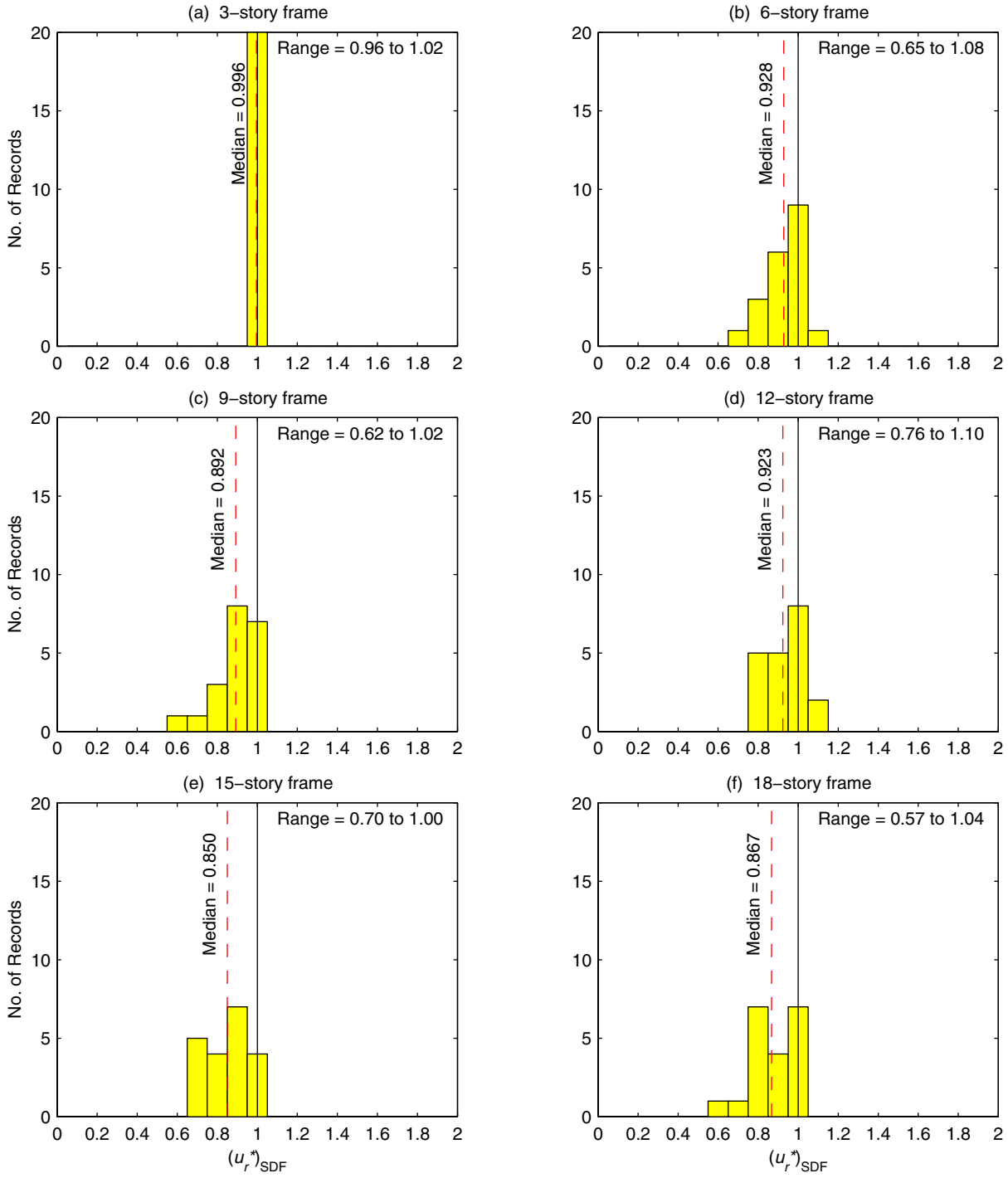

Fig. 2: **Histograms of ratio $\left(u_r^*\right)_{\text{SDF}}$ for generic elastic frames; range of values and median value of this ratio are noted.**

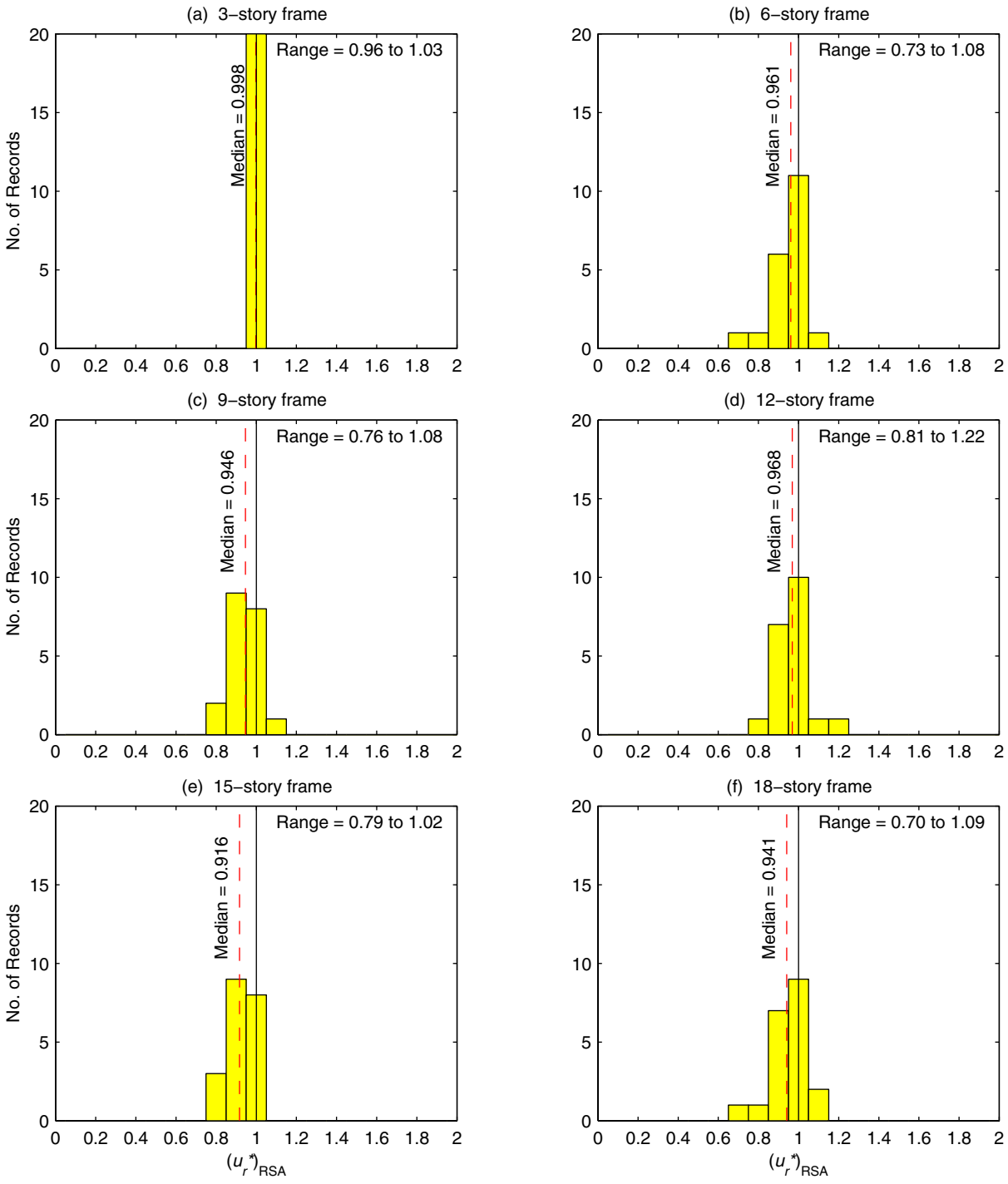

Fig. 3: **Histograms of ratio $\left(u_r^*\right)_{\text{RSA}}$ for generic elastic frames; range of values and median value of this ratio are noted.**

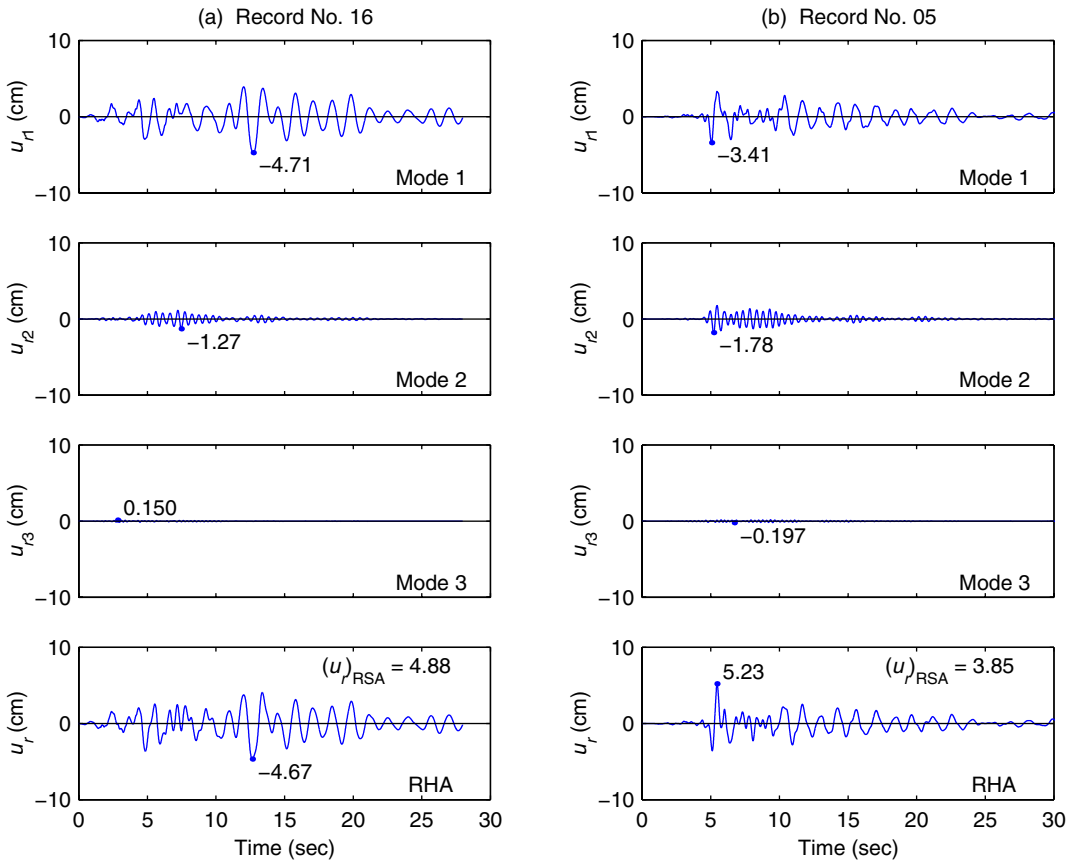

Fig. 4: **Modal contributions to roof displacement of elastic 6-story frame to LMSR ground motions: (a) Record No. 16 and (b) Record No. 5; RSA estimate of roof displacement is also noted.**

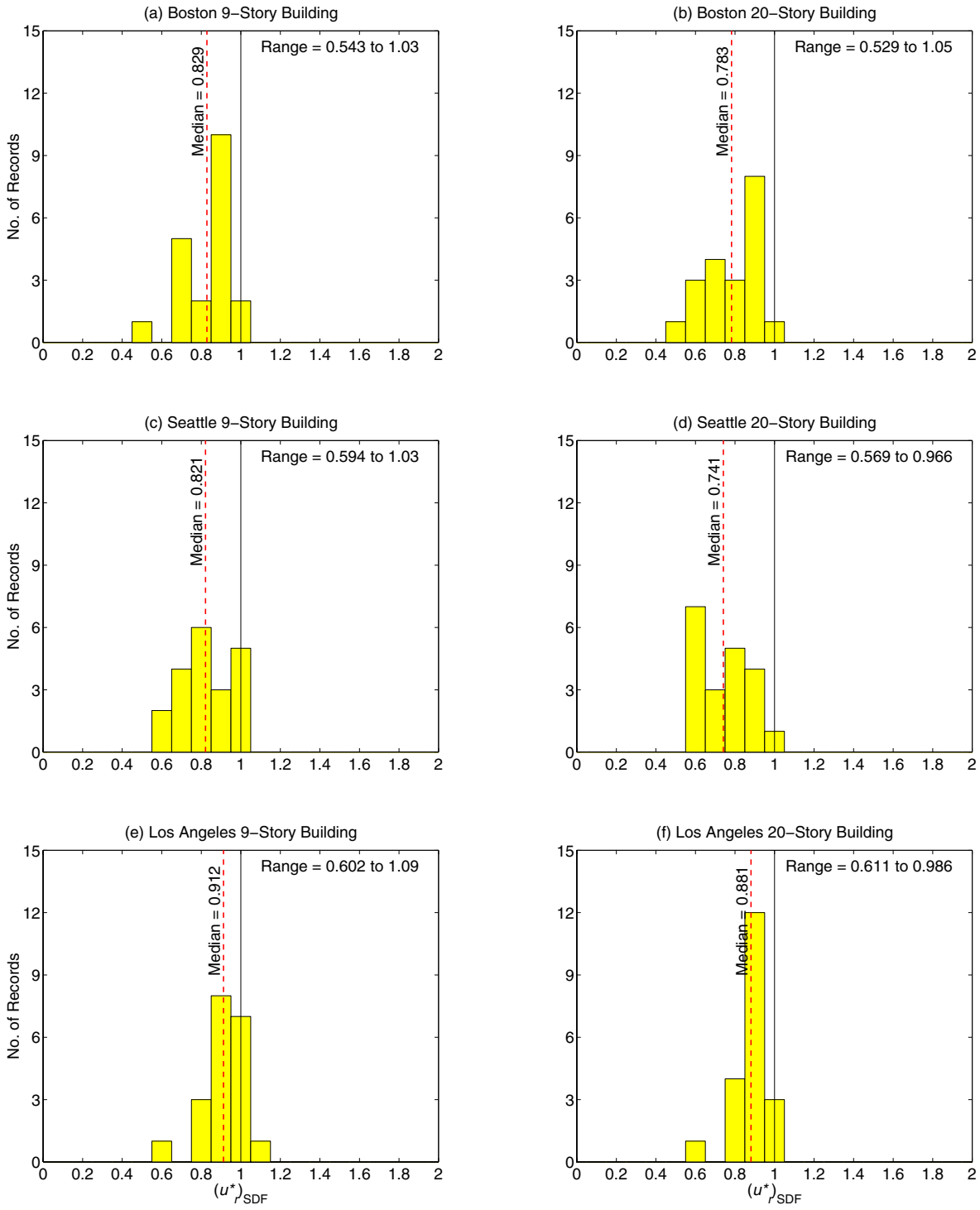

Fig. 5: **Histograms of ratio $\left(u_r^*\right)_{\mathrm{SDF}}$ for SAC buildings analyzed as elastic systems; range of values and median value of this ratio are noted.**

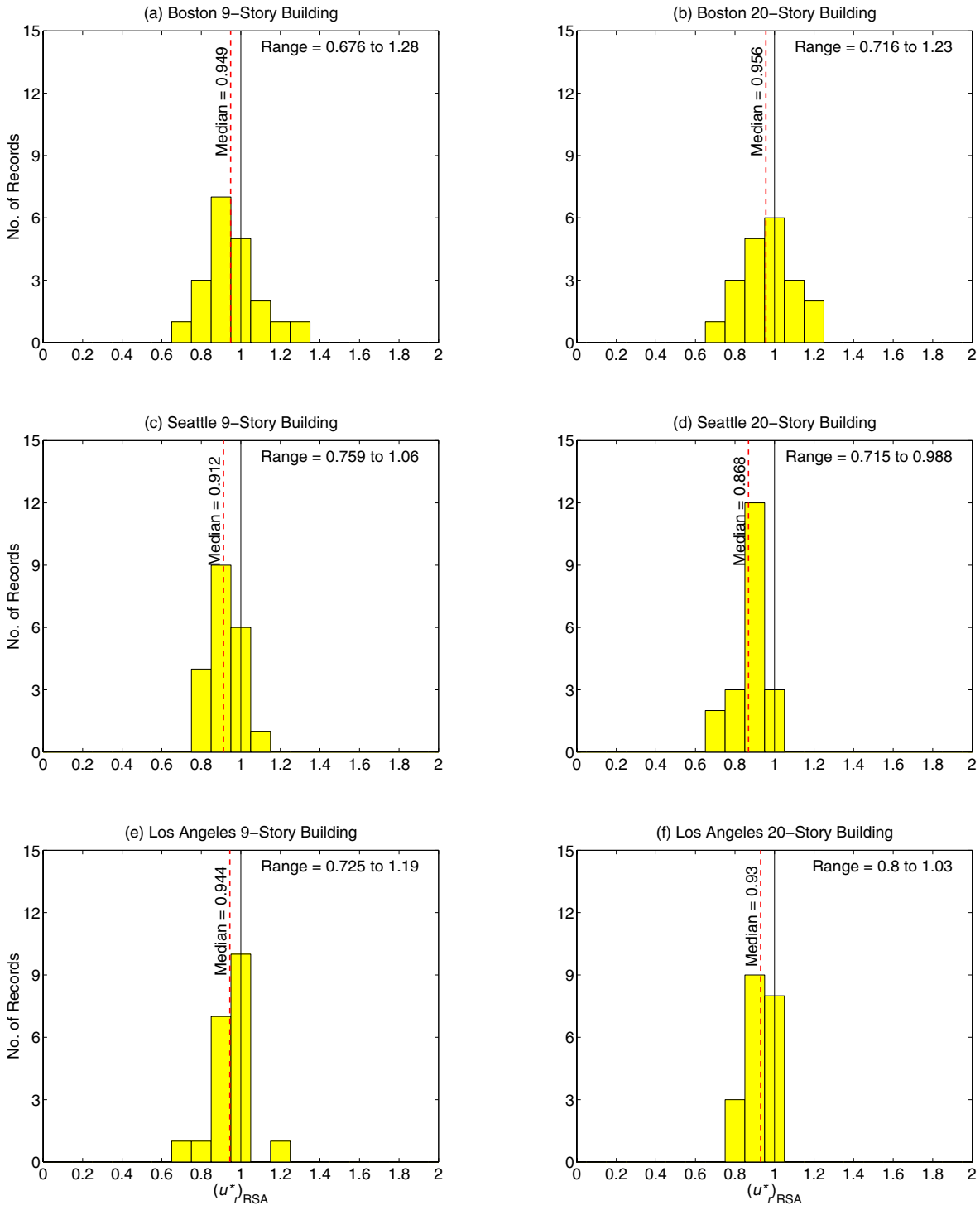

Fig. 6: **Histograms of ratio $\left(u_r^*\right)_{\text{RSA}}$ for SAC buildings analyzed as elastic systems; range of values and median value of this ratio are noted.**

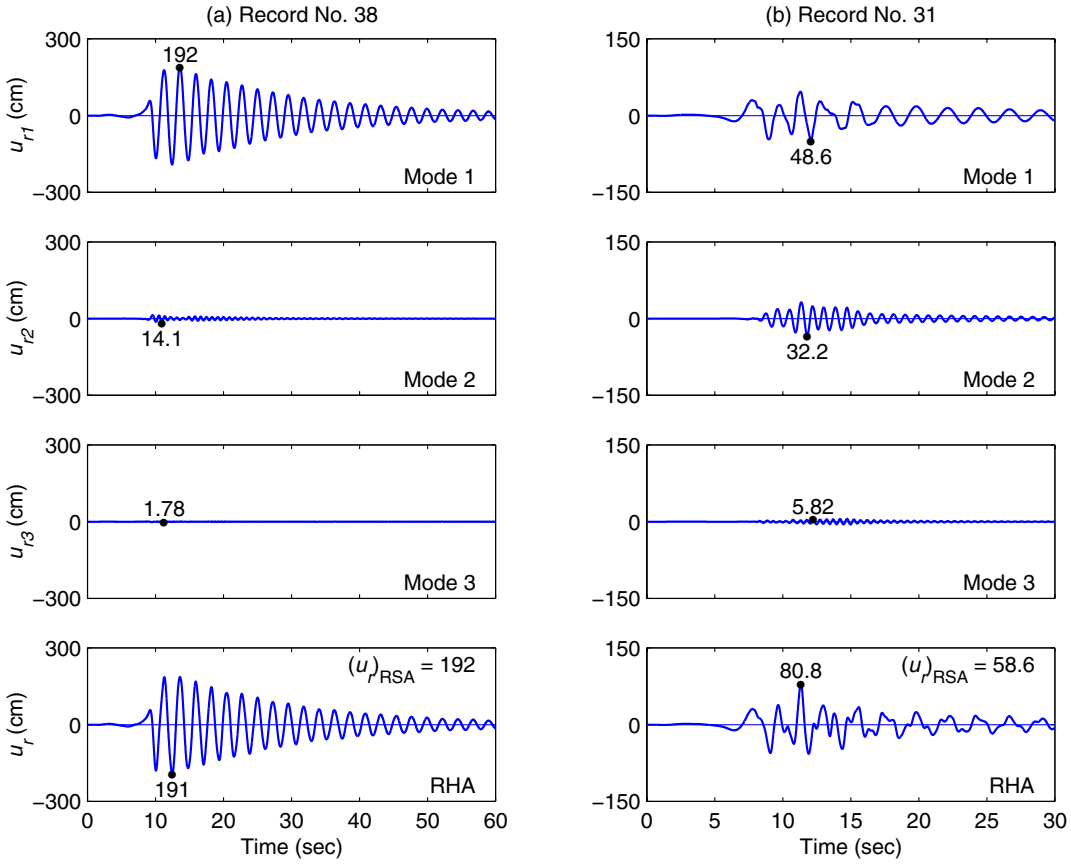

Fig. 7: **Modal contributions to roof displacement of Los Angeles 9-story building analyzed as an elastic system to SAC ground motions: (a) Record No. 38; (b) Record No. 31; RSA estimate of roof displacement is also noted.**

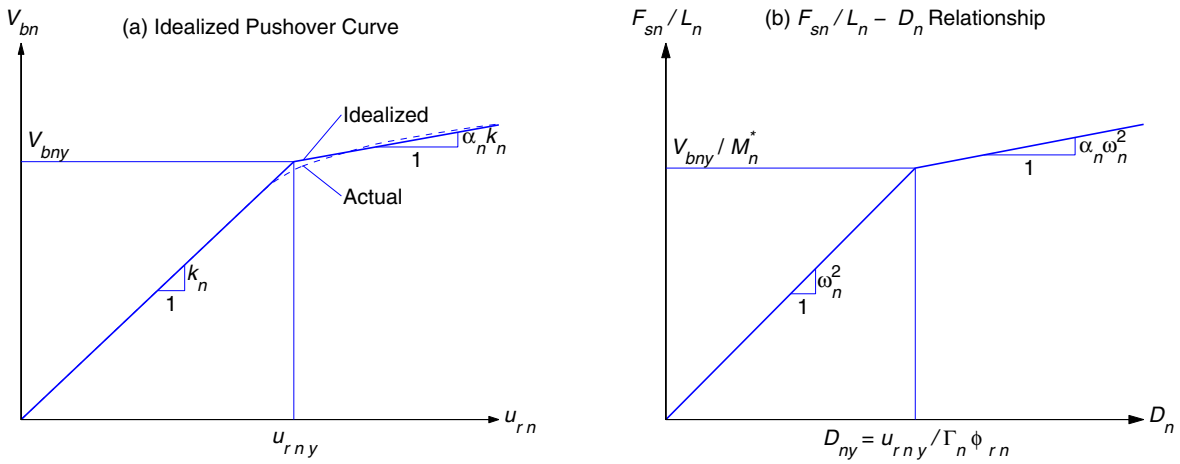

Fig. 8: Pushover curve and SDF system curve.

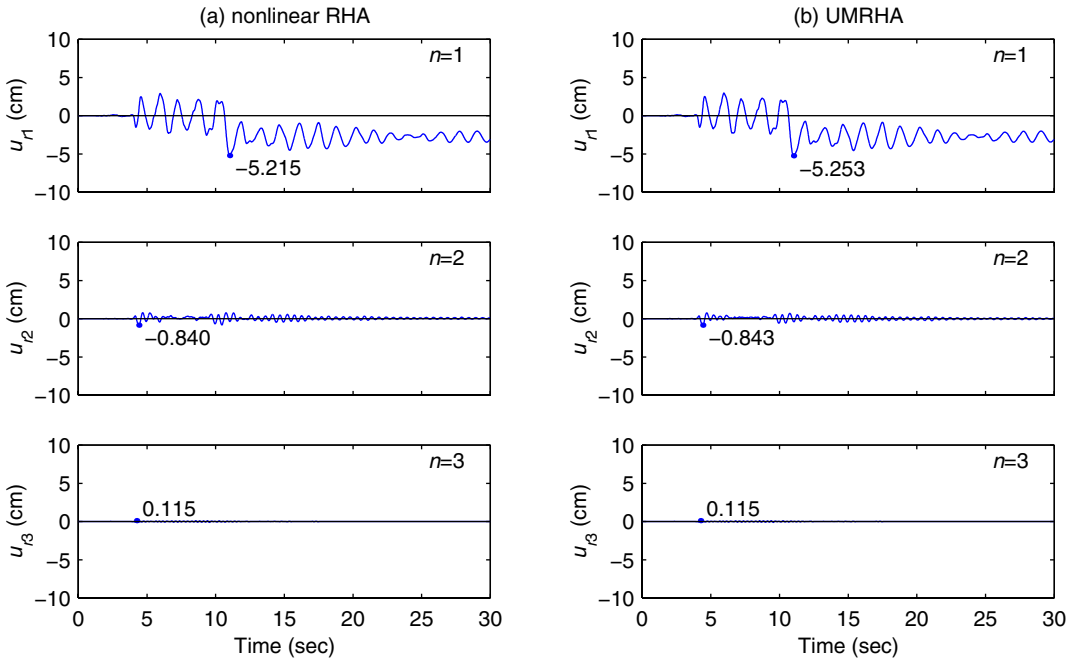

Fig. 9: Roof displacement of a 6-story frame $(\mu = 6)$ due to $\mathbf{p}_{\text{eff,n}}(t) = -\mathbf{s}_n \ddot{u}_g(t)$, *n* = 1,2, and 3, where $\ddot{u}_g(t)$ = LMSR Record No. 14 (a) "exact" solution by nonlinear RHA; and (b) approximate solution by UMRHA.

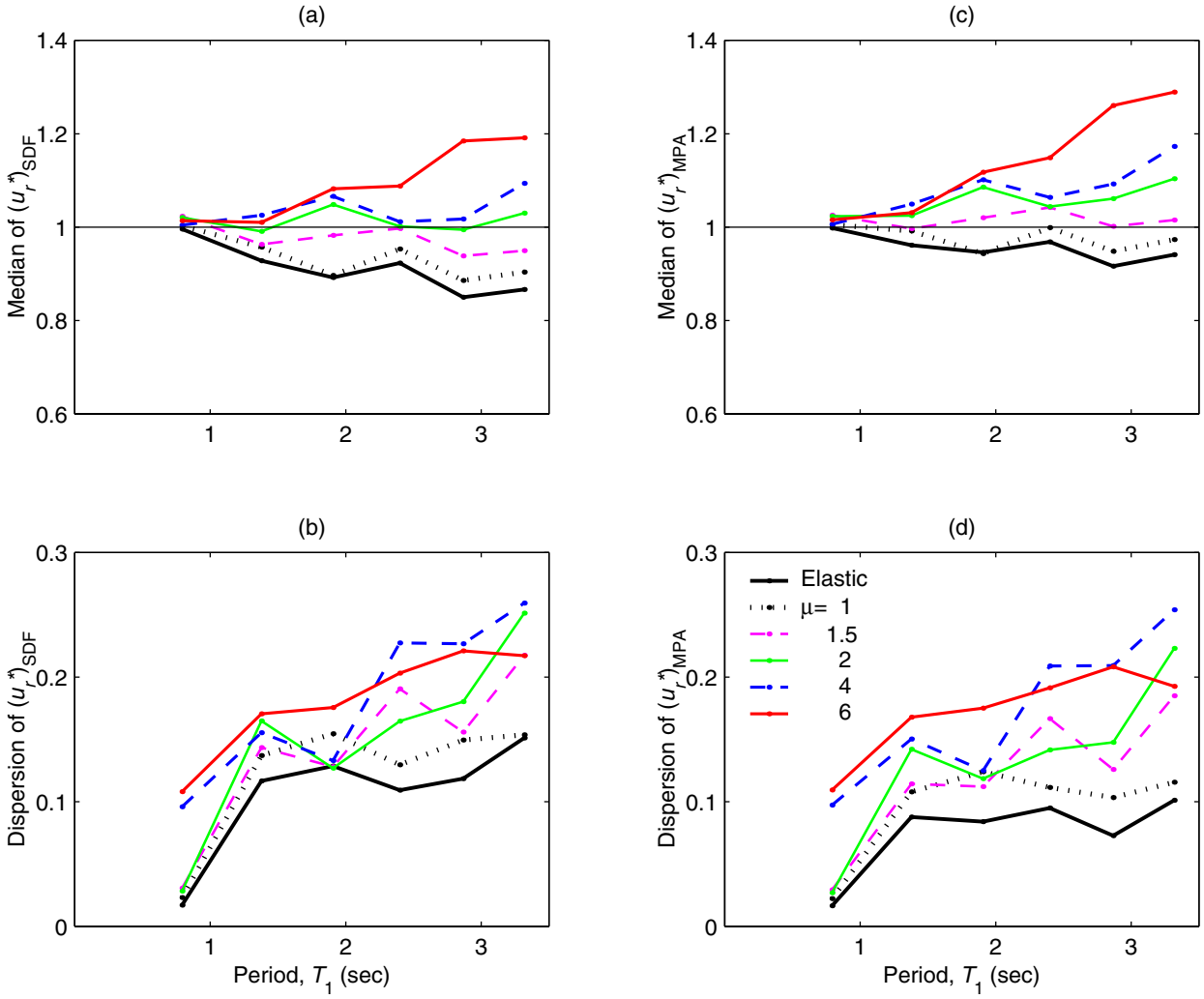

Fig. 10: **Median and dispersion of $\left(u_r^*\right)_{\text{SDF}}$ and $\left(u_r^*\right)_{\text{MPA}}$ versus fundamental vibration period T_1 for generic inelastic frames.**

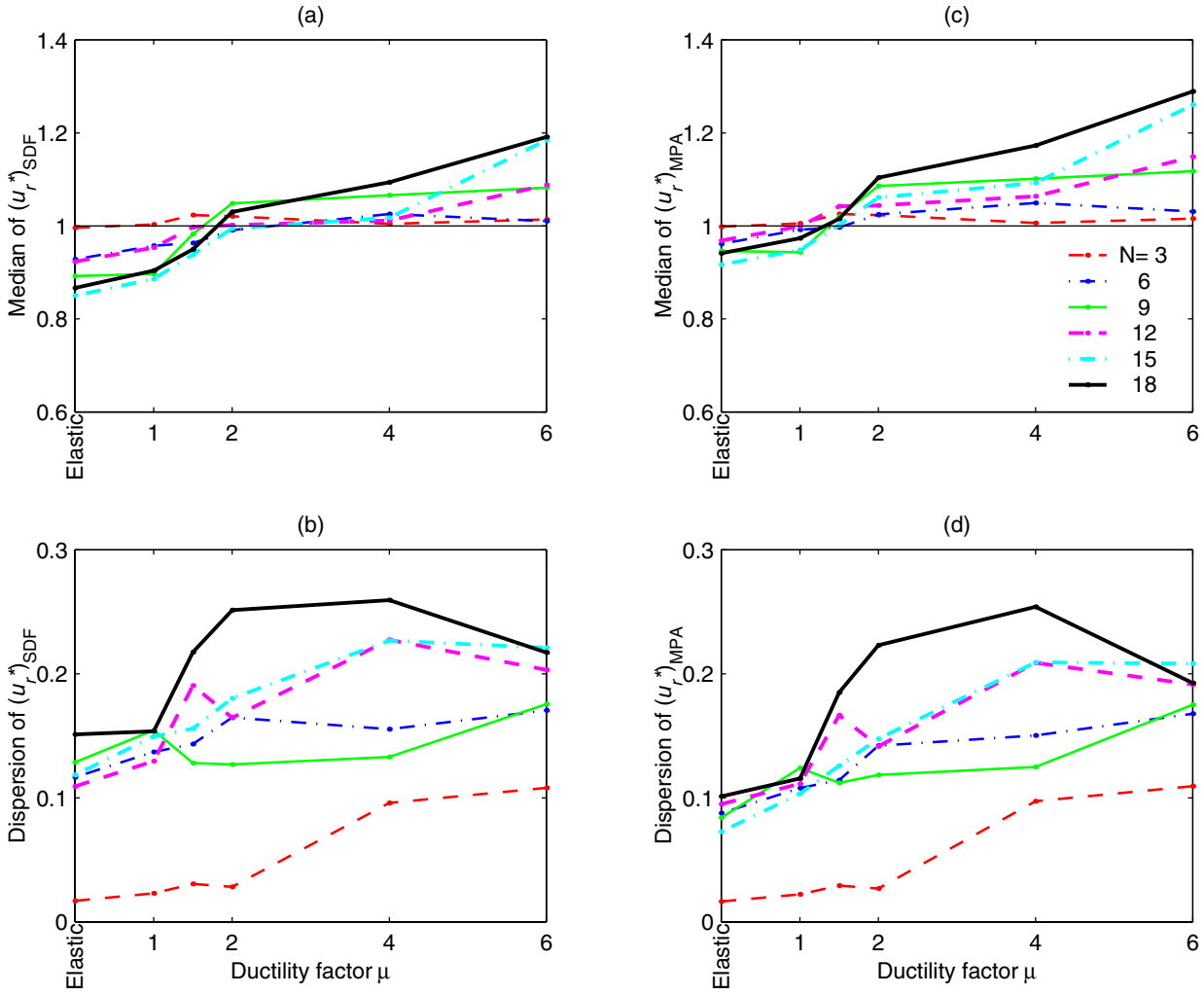

Fig. 11: **Median and dispersion of $\left(u_r^*\right)_{\text{SDF}}$ and $\left(u_r^*\right)_{\text{MPA}}$ versus μ for generic inelastic frames of 3, 6, 9, 12, 15, and 18 stories.**

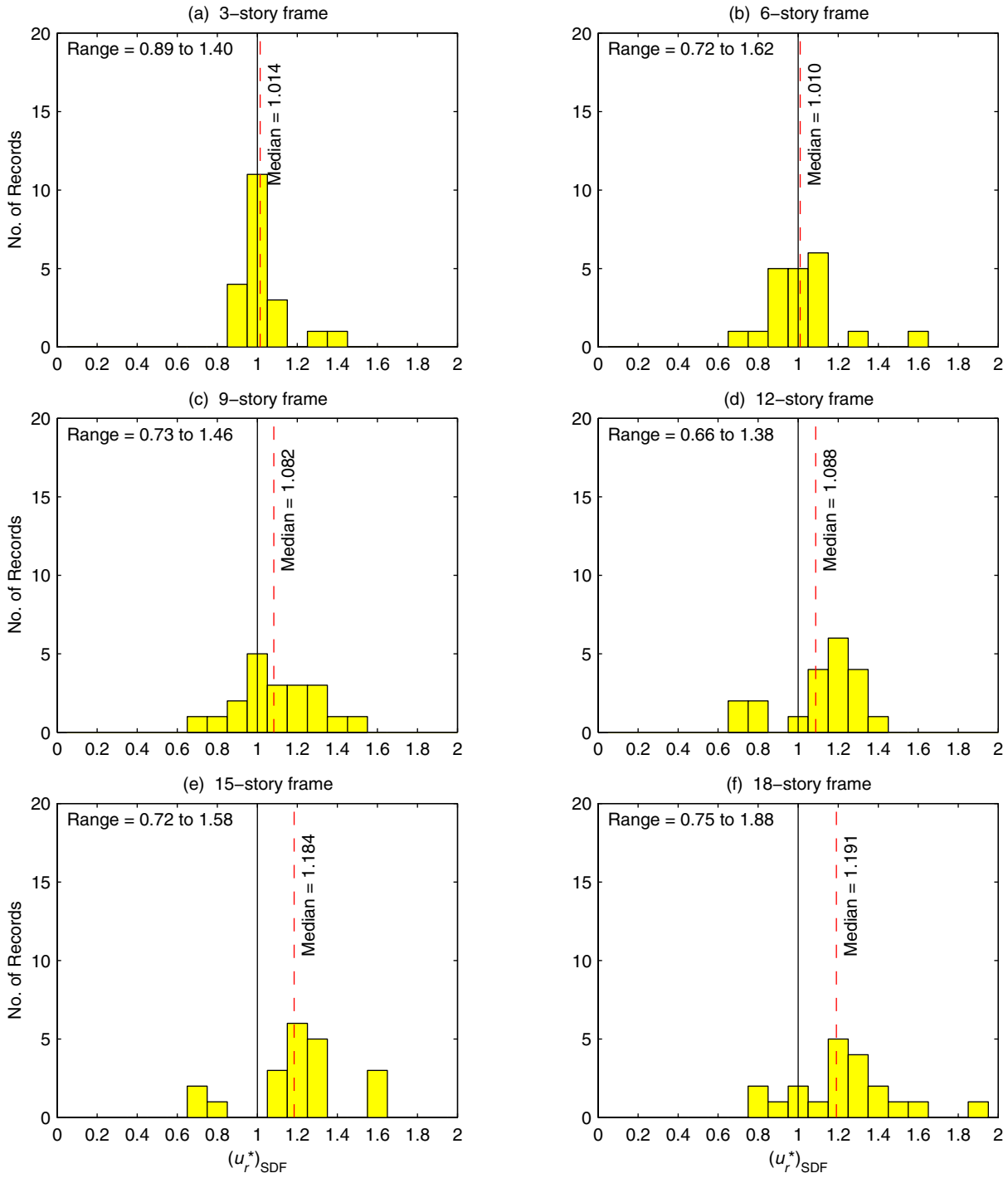

Fig. 12: Histograms of ratio $\left(u_r^*\right)_{\text{SDF}}$ for generic frames with design ductility factor $\mu = 6$; range of values and median value of this ratio are noted.

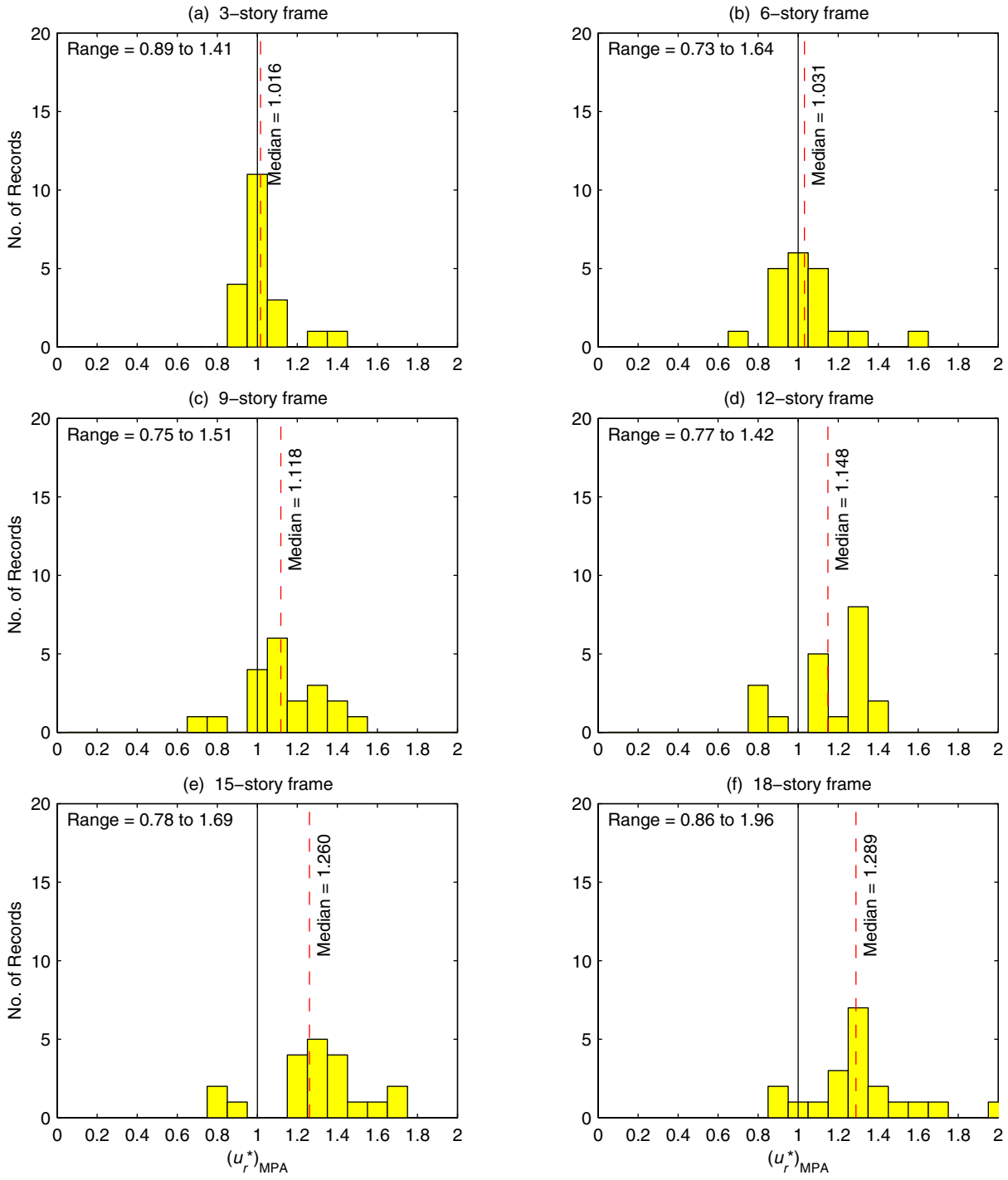

Fig. 13: Histograms of ratio $\left(u_r^*\right)_{\text{MPA}}$ for generic frames with design ductility factor $\mu = 6$; range of values and median value of this ratio are noted.

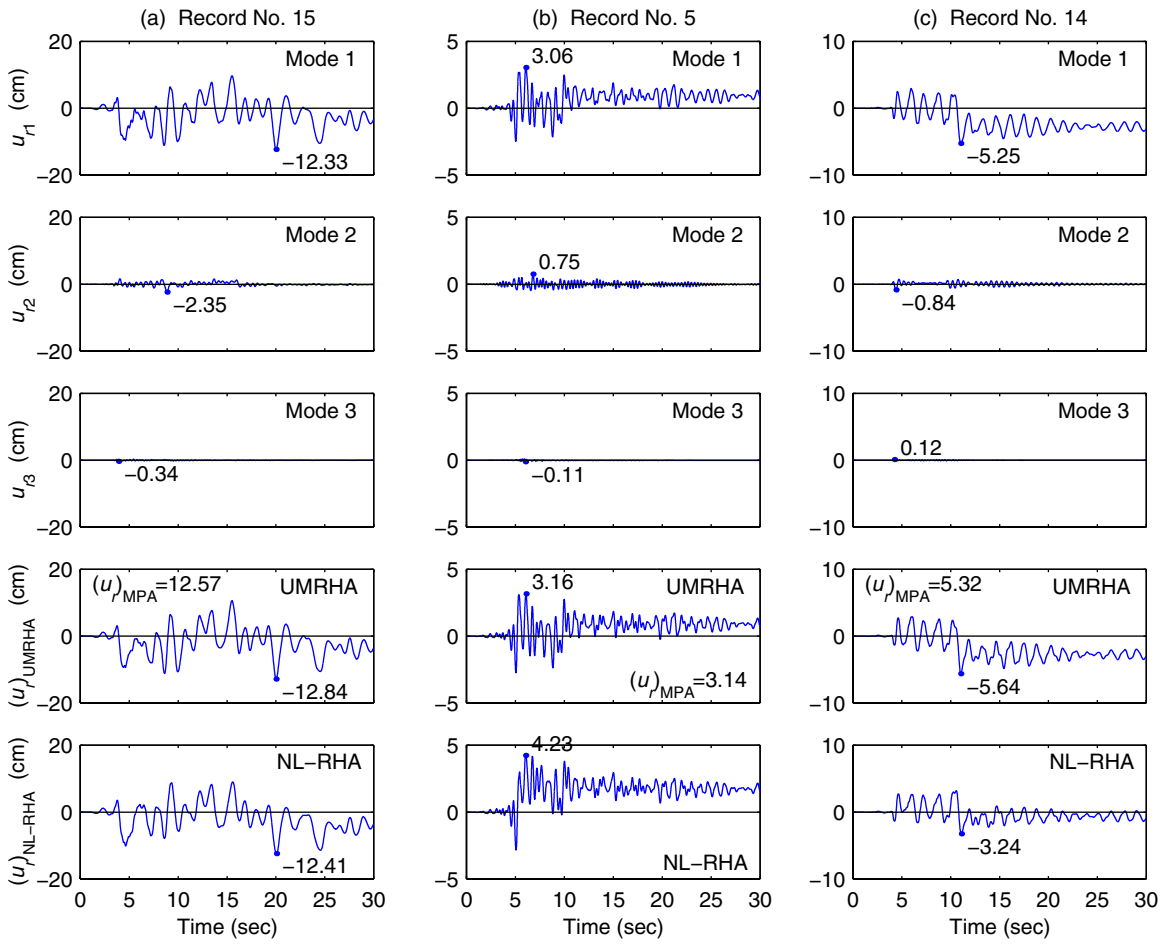

Fig. 14: **Response histories of roof displacement of a 6-story frame $(\mu = 6)$ due to three ground motions: individual "modal" responses, combined response from UMRHA, and "exact" response from nonlinear RHA; parts (a) and (c) are for frame with $T_1 = 0.045H^{0.8}$ and part (b) is for $T_1 = 0.028H^{0.8}$; MPA estimate of roof displacement is also noted.**

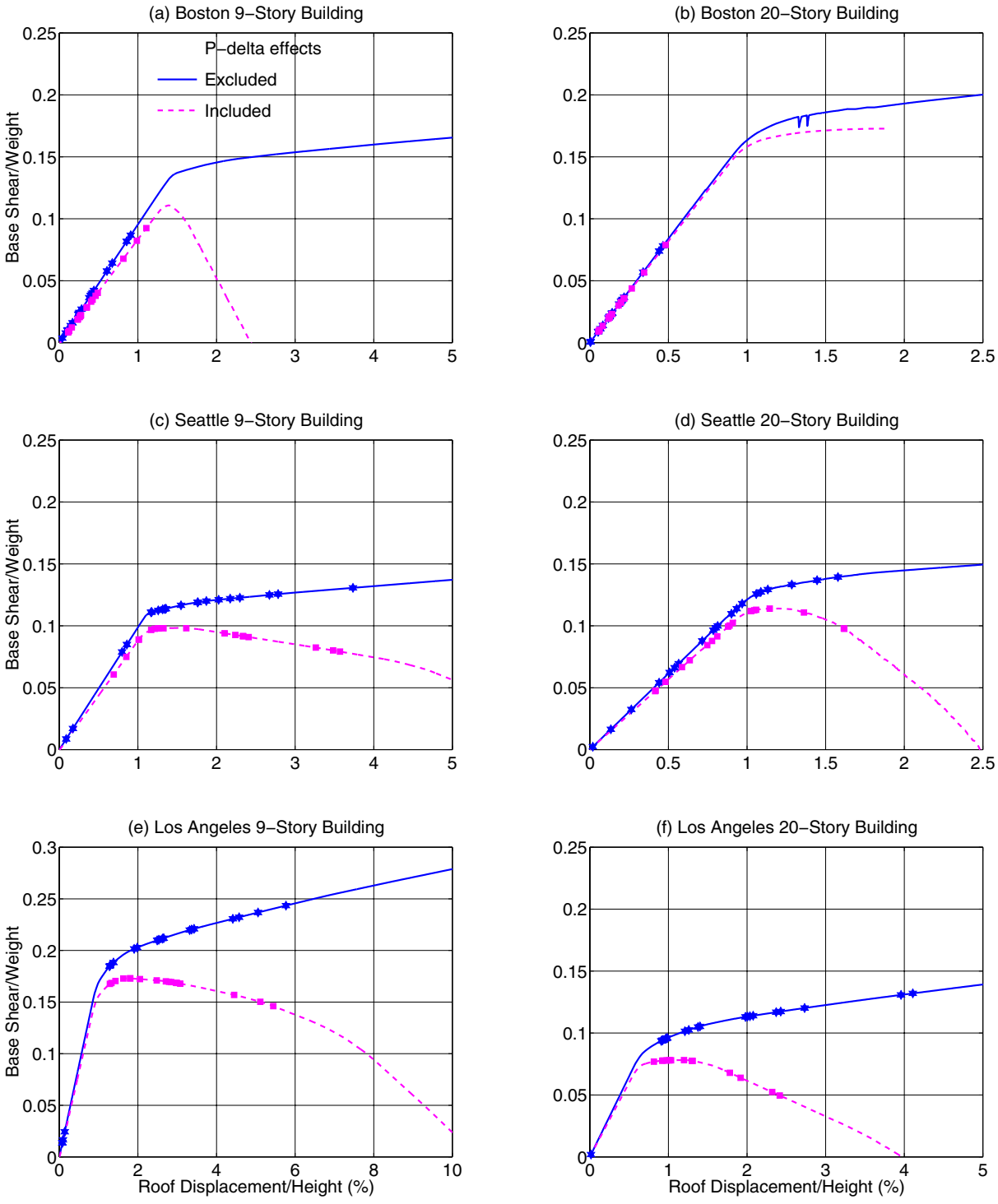

Fig. 15: First-"mode" pushover curves for SAC buildings for two cases: P-delta effects due to gravity loads excluded or included.

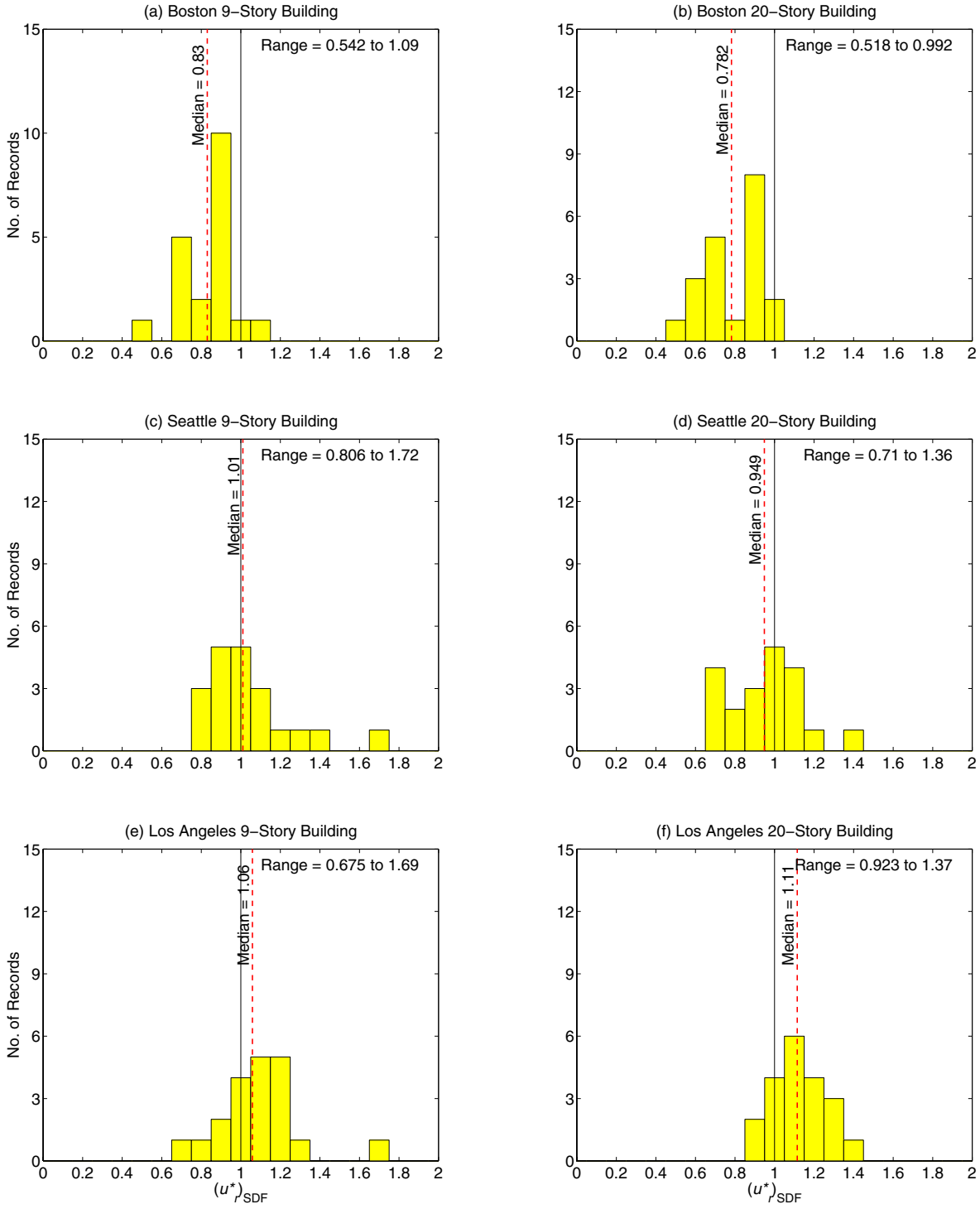

Fig. 16: Histograms of ratio $\left(u_r^*\right)_{\text{SDF}}$ for SAC buildings excluding P-delta effects due to gravity loads; range of values and median value of this ratio are noted.

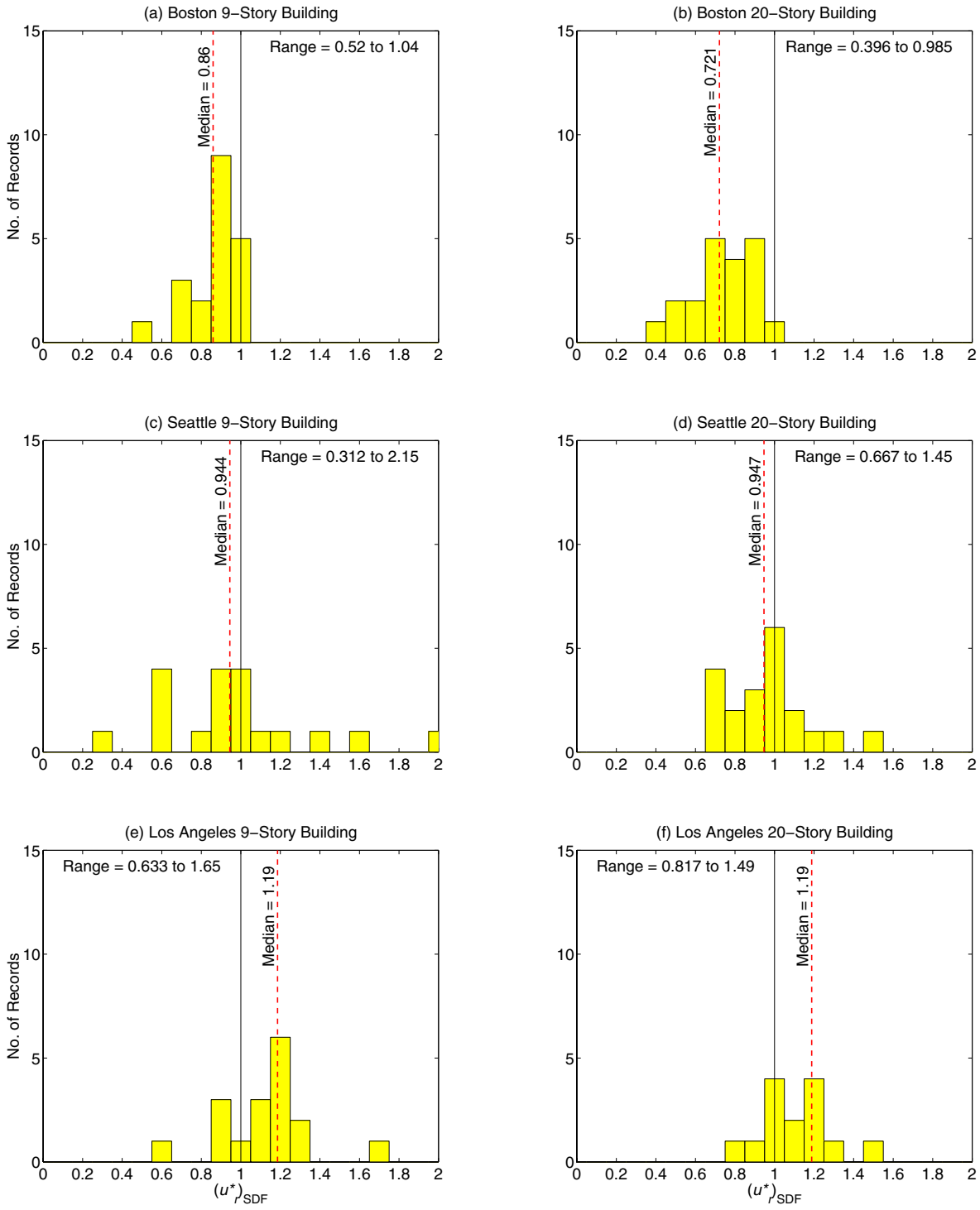

Fig. 17: Histograms of ratio $\left(u_r^*\right)_{\text{SDF}}$ for SAC buildings including P-delta effects due to gravity loads; range of values and median value of this ratio are noted.

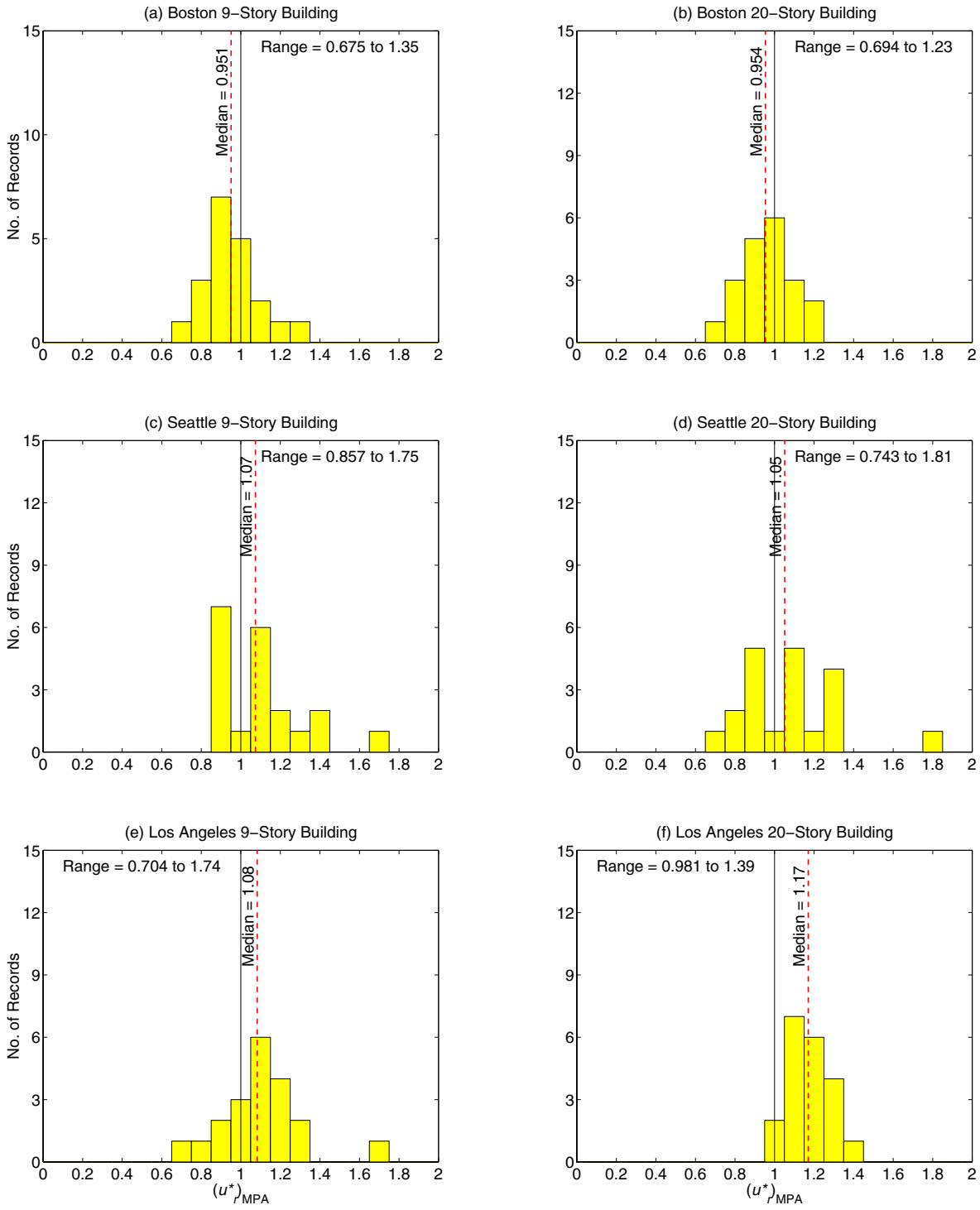

Fig. 18: Histograms of ratio $\left(u_r^*\right)_{\text{MPA}}$ for SAC buildings excluding P-delta effects due to gravity loads; range of values and median value of this ratio are noted.

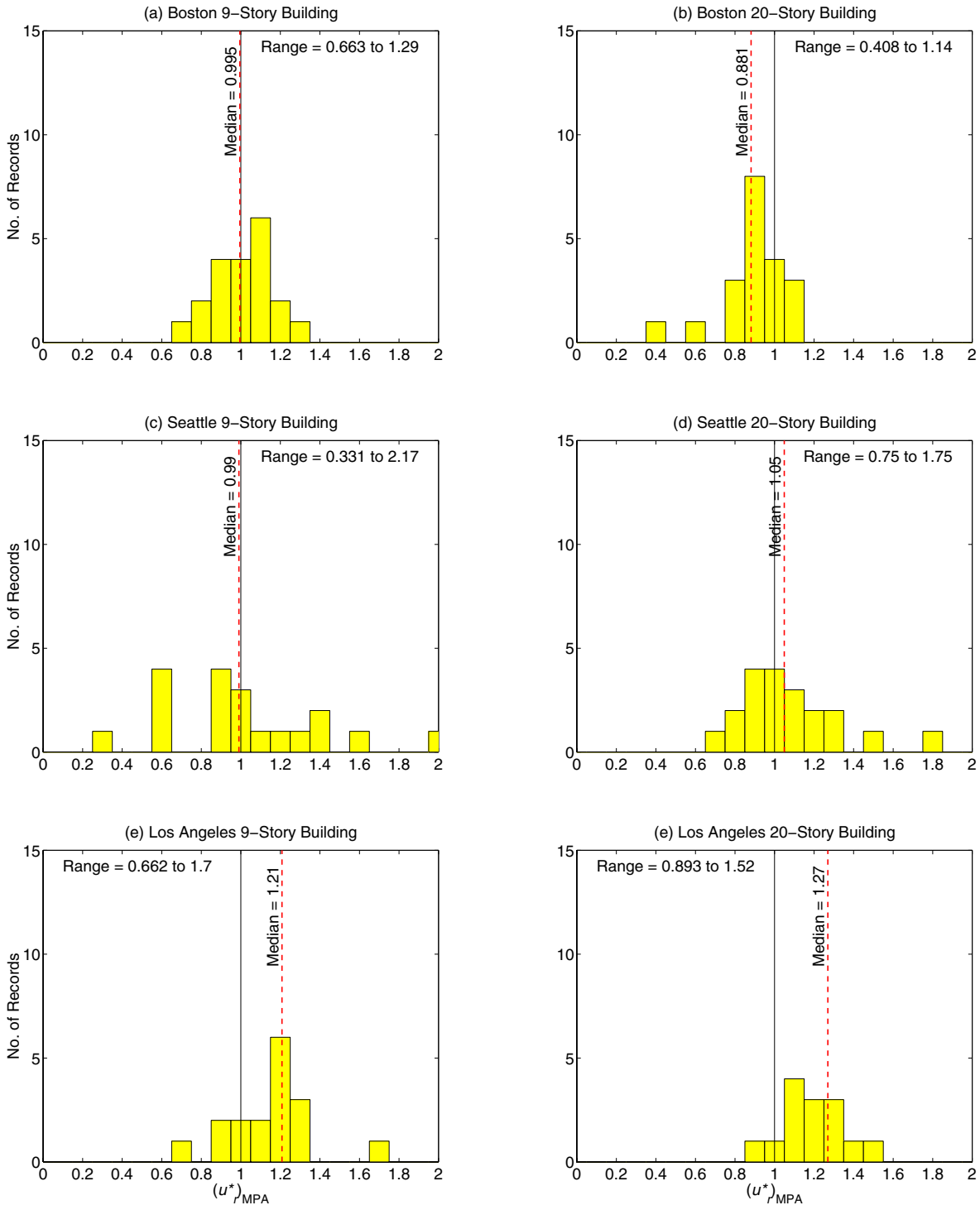

Fig. 19: Histograms of ratio $\left(u_r^*\right)_{\text{MPA}}$ SAC buildings including P-delta effects due to gravity loads; range of values and median value of this ratio are noted.

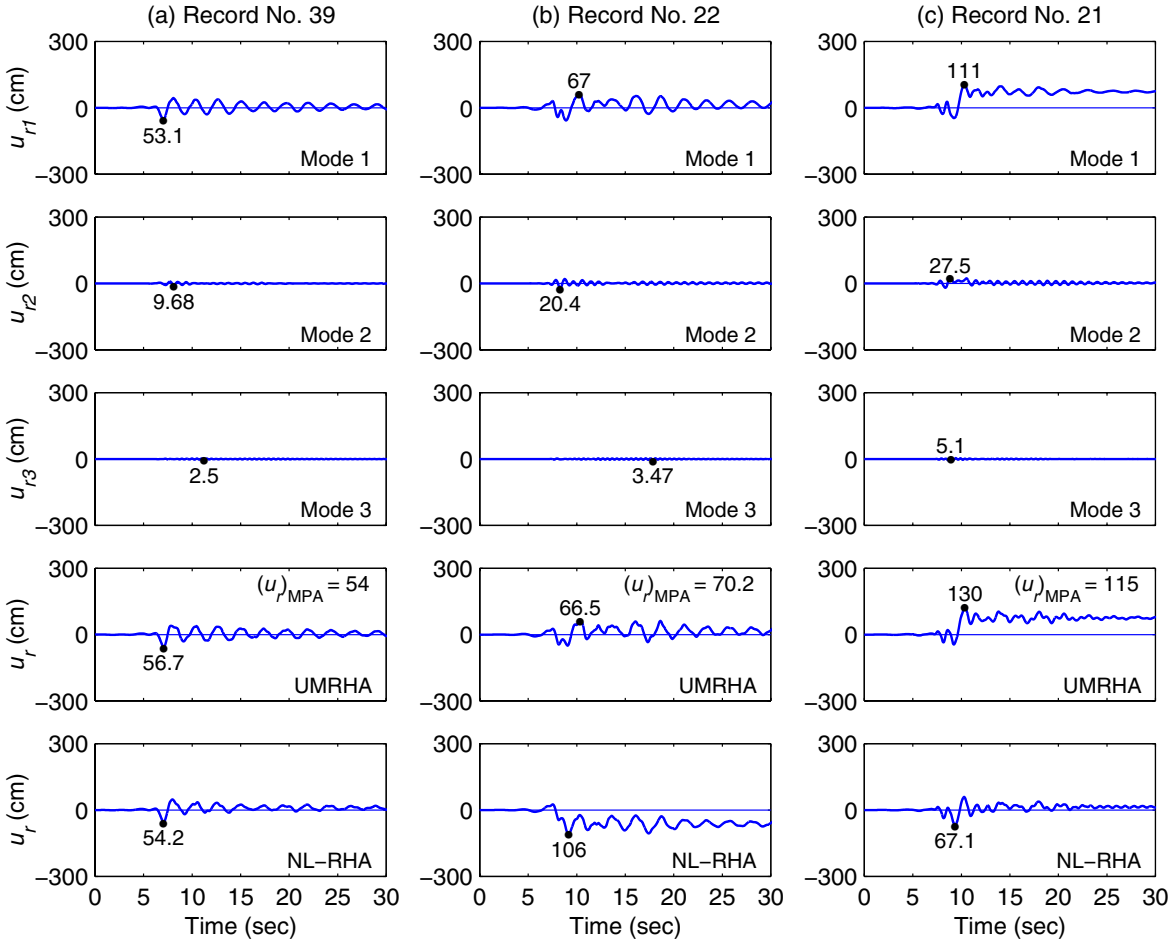

Fig. 20: **Response histories of roof displacement of Los Angeles 9-story building including P-delta effects due to gravity loads for three ground motions: individual "modal" responses, combined response from UMRHA, and "exact" response from nonlinear RHA; MPA estimate of roof displacement is also noted.**

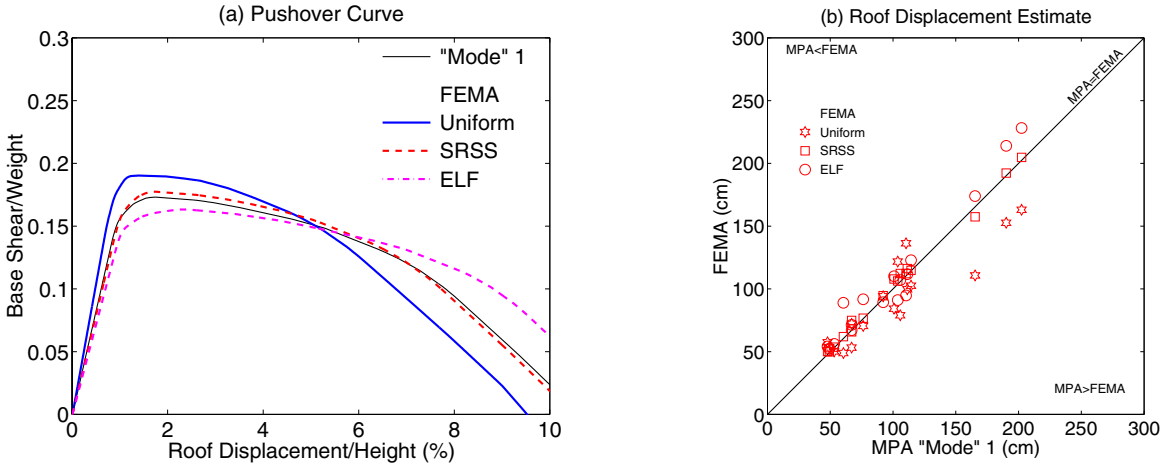

Fig. 21: **(a) Pushover curves for Los Angeles 9-story building associated with three FEMA-273 force distributions and the first-"mode" distribution; and (b) peak roof displacement from three FEMA SDF systems plotted against its value from the first-"mode" inelastic SDF system; P-delta effects due to gravity loads are included for all cases.**

PEER REPORTS

PEER reports are available from the National Information Service for Earthquake Engineering (NISEE). To order PEER reports, please contact the Pacific Earthquake Engineering Research Center, 1301 South 46th Street, Richmond, California 94804-4698. Tel.: (510) 231-9468; Fax: (510) 231-9461.

PEER 2001/16 *Statistics of SDF-System Estimate of Roof Displacement for Pushover Analysis of Buildings.* Anil K. Chopra, Rakesh K. Goel, and Chatpan Chintanapakdee. December 2001. $15.00

PEER 2001/12 *Development of Geotechnical Capabilities in OpenSees.* Boris Jeremic. September 2001. $13.00

PEER 2001/11 *Analytical and Experimental Study of Fiber-Reinforced Elastomeric Isolators*. James M. Kelly and Shakhzod M. Takhirov. September 2001. $15.00

PEER 2001/10 *Amplification Factors for Spectral Acceleration in Active Regions.* Jonathan P. Stewart, Andrew H. Liu, Yoojoong Choi, and Mehmet B. Baturay. December 2001. $20.00

PEER 2001/09 *Ground Motion Evaluation Procedures for Performance-Based Design.* Jonathan P. Stewart, Shyh-Jeng Chiou, Jonathan D. Bray, Robert W. Graves, Paul G. Somerville, and Norman A. Abrahamson. September 2001. $26.00

PEER 2001/08 *Experimental and Computational Evaluation of Reinforced Concrete Bridge Beam-Column Connections for Seismic Performance*. Clay J. Naito, Jack P. Moehle, and Khalid M. Mosalam. November 2001. $26.00

PEER 2001/07 *The Rocking Spectrum and the Shortcomings of Design Guidelines.* Nicos Makris and Dimitrios Konstantinidis. August 2001. $15.00

PEER 2001/06 *Development of an Electrical Substation Equipment Performance Database for Evaluation of Equipment Fragilities*. Thalia Agnanos. April 1999. $15.00

PEER 2001/05 *Stiffness Analysis of Fiber-Reinforced Elastomeric Isolators.* Hsiang-Chuan Tsai and James M. Kelly. May 2001. $20.00

PEER 2001/04 *Organizational and Societal Considerations for Performance-Based Earthquake Engineering.* Peter J. May. April 2001. $15.00

PEER 2001/03 *A Modal Pushover Analysis Procedure to Estimate Seismic Demands for Buildings: Theory and Preliminary Evaluation.* Anil K. Chopra and Rakesh K. Goel. January 2001. $15.00

PEER 2001/02 *Seismic Response Analysis of Highway Overcrossings Including Soil-Structure Interaction.* Jian Zhang and Nicos Makris. March 2001. $20.00

PEER 2001/01 *Experimental Study of Large Seismic Steel Beam-to-Column Connections.* Egor P. Popov and Shakhzod M. Takhirov. November 2000. $15.00

PEER 2000/10 *The Second U.S.-Japan Workshop on Performance-Based Earthquake Engineering Methodology for Reinforced Concrete Building Structures.* March 2000. $39.00

PEER 2000/09 *Structural Engineering Reconnaissance of the August 17, 1999 Earthquake: Kocaeli (Izmit), Turkey.* Halil Sezen, Kenneth J. Elwood, Andrew S. Whittaker, Khalid Mosalam, John J. Wallace, and John F. Stanton. December 2000. $20.00

PEER 2000/08 *Behavior of Reinforced Concrete Bridge Columns Having Varying Aspect Ratios and Varying Lengths of Confinement.* Anthony J. Calderone, Dawn E. Lehman, and Jack P. Moehle. January 2001. $20.00

PEER 2000/07 *Cover-Plate and Flange-Plate Reinforced Steel Moment-Resisting Connections.* Taejin Kim, Andrew S. Whittaker, Amir S. Gilani, Vitelmo V. Bertero, and Shakhzod M. Takhirov. September 2000. $33.00

PEER 2000/06 *Seismic Evaluation and Analysis of 230-kV Disconnect Switches.* Amir S. J. Gilani, Andrew S. Whittaker, Gregory L. Fenves, Chun-Hao Chen, Henry Ho, and Eric Fujisaki. July 2000. $26.00

PEER 2000/05 *Performance-Based Evaluation of Exterior Reinforced Concrete Building Joints for Seismic Excitation.* Chandra Clyde, Chris P. Pantelides, and Lawrence D. Reaveley. July 2000. $15.00

PEER 2000/04 *An Evaluation of Seismic Energy Demand: An Attenuation Approach.* Chung-Che Chou and Chia-Ming Uang. July 1999. $20.00

PEER 2000/03 *Framing Earthquake Retrofitting Decisions: The Case of Hillside Homes in Los Angeles.* Detlof von Winterfeldt, Nels Roselund, and Alicia Kitsuse. March 2000. $13.00

PEER 2000/02 *U.S.-Japan Workshop on the Effects of Near-Field Earthquake Shaking.* Andrew Whittaker, ed. July 2000. $20.00

PEER 2000/01 *Further Studies on Seismic Interaction in Interconnected Electrical Substation Equipment.* Armen Der Kiureghian, Kee-Jeung Hong, and Jerome L. Sackman. November 1999. $20.00

PEER 1999/14 *Seismic Evaluation and Retrofit of 230-kV Porcelain Transformer Bushings*. Amir S. Gilani, Andrew S. Whittaker, Gregory L. Fenves, and Eric Fujisaki. December 1999. $26.00

PEER 1999/13 *Building Vulnerability Studies: Modeling and Evaluation of Tilt-up and Steel Reinforced Concrete Buildings.* John W. Wallace, Jonathan P. Stewart, and Andrew S. Whittaker, editors. December 1999. $26.00

PEER 1999/12 *Rehabilitation of Nonductile RC Frame Building Using Encasement Plates and Energy-Dissipating Devices.* Mehrdad Sasani, Vitelmo V. Bertero, James C. Anderson. December 1999. $26.00

PEER 1999/11 *Performance Evaluation Database for Concrete Bridge Components and Systems under Simulated Seismic Loads.* Yael D. Hose and Frieder Seible. November 1999. $20.00

PEER 1999/10 *U.S.-Japan Workshop on Performance-Based Earthquake Engineering Methodology for Reinforced Concrete Building Structures.* December 1999. $33.00

PEER 1999/09 *Performance Improvement of Long Period Building Structures Subjected to Severe Pulse-Type Ground Motions*. James C. Anderson, Vitelmo V. Bertero, and Raul Bertero. October 1999. $26.00

PEER 1999/08 *Envelopes for Seismic Response Vectors.* Charles Menun and Armen Der Kiureghian. July 1999. $26.00

PEER 1999/07 *Documentation of Strengths and Weaknesses of Current Computer Analysis Methods for Seismic Performance of Reinforced Concrete Members.* William F. Cofer. November 1999. $15.00

PEER 1999/06 *Rocking Response and Overturning of Anchored Equipment under Seismic Excitations.* Nicos Makris and Jian Zhang. November 1999. $15.00

PEER 1999/05 *Seismic Evaluation of 550 kV Porcelain Transformer Bushings.* Amir S. Gilani, Andrew S. Whittaker, Gregory L. Fenves, and Eric Fujisaki. October 1999. $15.00

PEER 1999/04 *Adoption and Enforcement of Earthquake Risk-Reduction Measures.* Peter J. May, Raymond J. Burby, T. Jens Feeley, and Robert Wood. $15.00

PEER 1999/03 *Task 3 Characterization of Site Response General Site Categories*. Adrian Rodriguez-Marek, Jonathan D. Bray, and Norman Abrahamson. February 1999. $20.00

PEER 1999/02 *Capacity-Demand-Diagram Methods for Estimating Seismic Deformation of Inelastic Structures: SDF Systems*. Anil K. Chopra and Rakesh Goel. April 1999. $15.00

PEER 1999/01 *Interaction in Interconnected Electrical Substation Equipment Subjected to Earthquake Ground Motions.* Armen Der Kiureghian, Jerome L. Sackman, and Kee-Jeung Hong. February 1999. $20.00

PEER 1998/08 *Behavior and Failure Analysis of a Multiple-Frame Highway Bridge in the 1994 Northridge Earthquake.* Gregory L. Fenves and Michael Ellery. December 1998. $20.00

PEER 1998/07 *Empirical Evaluation of Inertial Soil-Structure Interaction Effects.* Jonathan P. Stewart, Raymond B. Seed, and Gregory L. Fenves. November 1998. $26.00

PEER 1998/06 *Effect of Damping Mechanisms on the Response of Seismic Isolated Structures.* Nicos Makris and Shih-Po Chang. November 1998. $15.00

PEER 1998/05 *Rocking Response and Overturning of Equipment under Horizontal Pulse-Type Motions.* Nicos Makris and Yiannis Roussos. October 1998. $15.00

PEER 1998/04 *Pacific Earthquake Engineering Research Invitational Workshop Proceedings, May 14–15, 1998: Defining the Links between Planning, Policy Analysis, Economics and Earthquake Engineering.* Mary Comerio and Peter Gordon. September 1998. $15.00

PEER 1998/03 *Repair/Upgrade Procedures for Welded Beam to Column Connections.* James C. Anderson and Xiaojing Duan. May 1998. $33.00

PEER 1998/02 *Seismic Evaluation of 196 kV Porcelain Transformer Bushings.* Amir S. Gilani, Juan W. Chavez, Gregory L. Fenves, and Andrew S. Whittaker. May 1998. $20.00

PEER 1998/01 *Seismic Performance of Well-Confined Concrete Bridge Columns.* Dawn E. Lehman and Jack P. Moehle. December 2000. $33.00